Veterinär-Anatomisches Institut der Vetsuisse-Fakultät Universität Zürich

Direktor ad interim: Prof. Dr. B. Spiess
Arbeit unter Leitung von Prof. Dr. Peter Wild

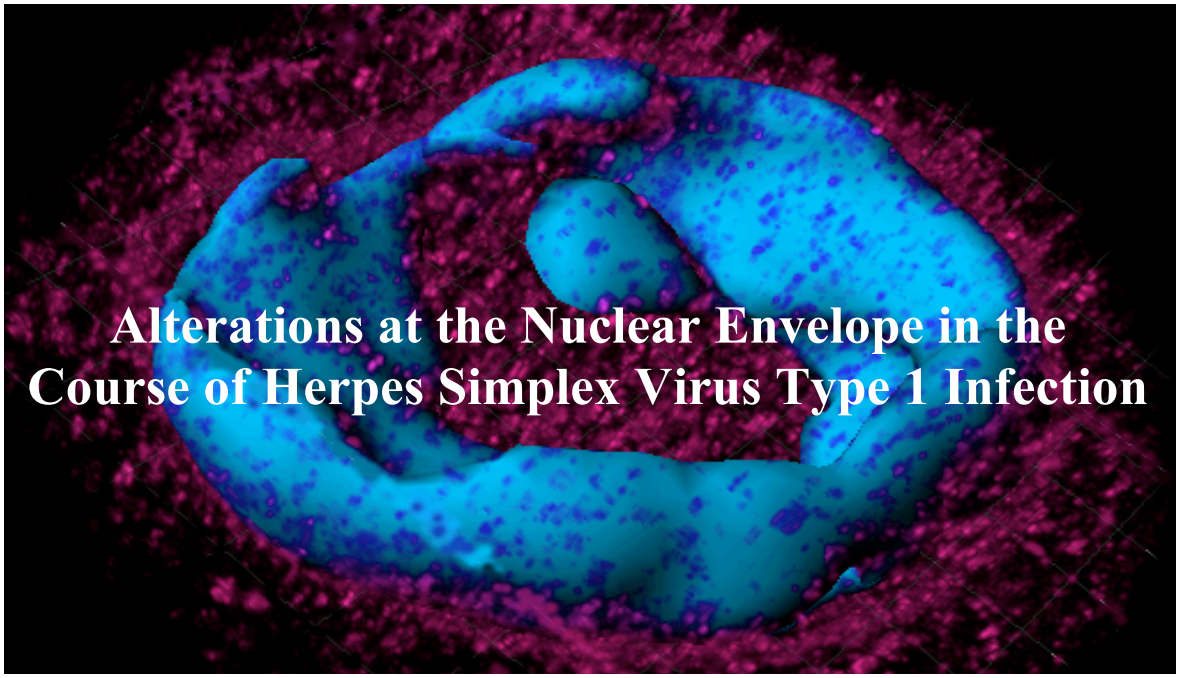

# Alterations at the Nuclear Envelope in the Course of Herpes Simplex Virus Type 1 Infection

**Inaugural-Dissertation**

zur Erlangung der Doktorwürde
der Vetsuisse-Fakultät Universität Zürich

vorgelegt von

**Céline Lorraine Manera**

Tierärztin
von Lausanne, VD

genehmigt auf Antrag von

Prof. Dr. P. Wild, Referent

Prof. Dr. M. Ackermann, Korreferent

Zürich 2007

**CONTENT**

# 1. ABSTRACT

Herpes viruses are composed of capsid, tegument and envelope. Capsids assemble in the nucleus. They exit the nucleus by budding at the inner nuclear membrane. This study focuses on the changes at the nuclear envelope in the course of herpes simplex virus 1 infection (HSV-1) of HeLa cells and Vero cells employing preparation techniques at ambient and low temperatures for high-resolution scanning- and transmission electron microscopy and confocal laser scanning microscopy. Examination of *in situ* prepared nuclei at ambient temperature revealed enlargement of nuclear pore channels from 20 nm in mock infected cells to 133 nm in HSV-1 infected cells, and an overall enlargement of nuclear pores up to 290 nm. The number of nuclear pores per 1 $\mu m^2$ decreased from 29.07 nuclear pores in mock infected cells to 6.47 nuclear pores in HSV-1 infected cells. Nuclear pore impairment was confirmed by transmission electron microscopy and by low temperature scanning electron microscopy. Changes in distribution of nuclear pores were also found by confocal microscopy. Determination of the area between nuclear pores prior to infection revealed that it is 10 times less than required for budding of a single capsid leading to the conclusion that nuclear membranes must be provided either by de novo synthesis or by dislocation from other cellular sites.

# 2. INTRODUCTION

The nuclear envelope divides eukaryotic cells into a nuclear and a cytoplasmic compartment. It comprises two lipid bilayers, the inner and the outer nuclear membrane. Local fusions between both membranes create giant aqueous channels (nuclear pores), through which all nucleocytoplasmic exchanges proceed. These pores are embedded into elaborate protein structures of eightfold rotational symmetry called the nuclear pore complexes (NPCs, Fig. 1) (Suntharalingam 2003; Wozniak 2003; Drummond 2004).

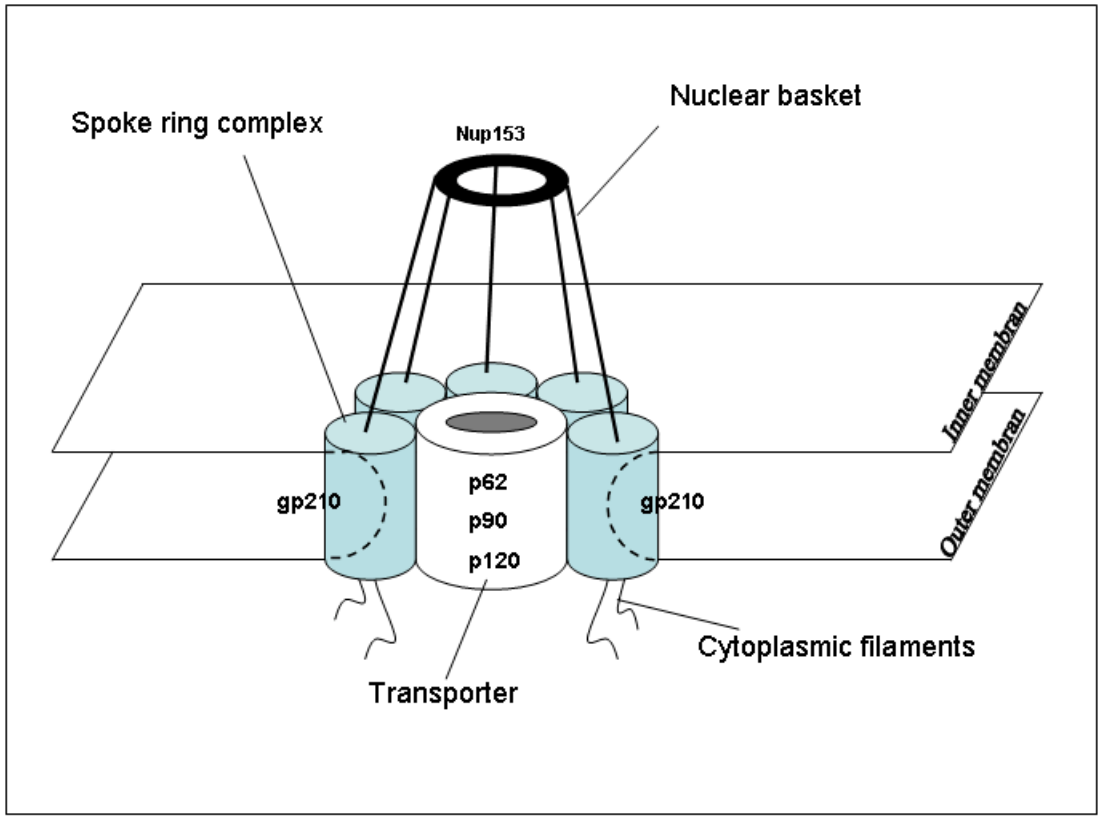


**Fig. 1.** Schematic drawing of a nuclear pore complex showing the localization of nuclear pore proteins gp210, p62, p90, p120 and Nup153.

Herpes virions (Fig. 2) consist of more than 30 virally encoded proteins which are present in four morphologically distinct components (Roizman 2001). The inner core contains the viral genomic double-stranded DNA which is enclosed in an icosahedral (T=16) capsid. The capsid is surrounded by an amorphous protein

layer, termed the tegument, which is bounded by an envelope derived from host cell membrane. After viral gene expression and DNA synthesis, capsid proteins are translocated from the cytoplasm to the nucleus where they assemble autocatalytically to capsids which then package DNA in a process that resembles head assembly and DNA packaging in bacteriophages (Braines 2005). The tegument contains import and regulatory proteins that are released into the newly infected cells following fusion of the virion envelope with the host cell plasma membrane. While the functions of many of the tegument proteins have yet to be precisely defined, several have been shown to aid in the initiation of the viral replicative cycle (e.g. VP16) (Roizman 1996). The envelope consists of a bilayer. This bilayer membrane is visualized as a continuous smoothly curved surface, about 5 nm thick. The diameter of virions ranged from 170 to 200 nm, averaging 186 nm. An array of glycoproteins protrudes from each virion, making the full diameter, on average about 225 nm. Distribution of the 11 glycoproteins, as for example gB, gC, gD has been studied by electron tomography that revealed 595-578 glycoproteins per virions (Grunewald, Desai et al. 2003).

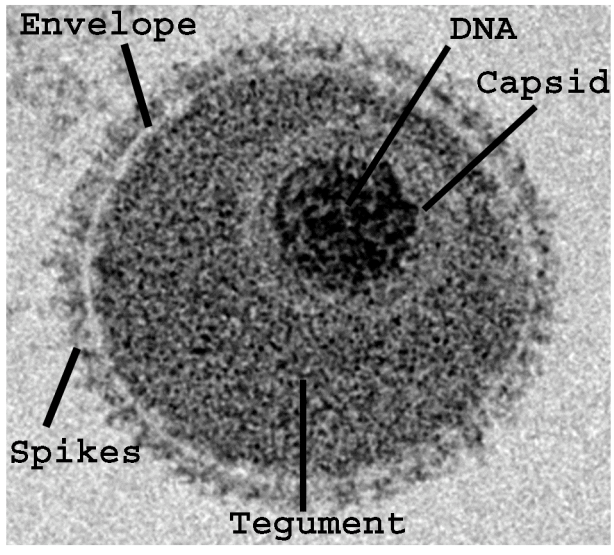


**Fig. 2.** Transmission electron microscopic image of a HSV-1 particle showing all constituents in great detail like all members of the herpesvirus family.

Herpes simplex virus 1 (HSV-1) replicates in the nucleus of host cells and radically alters nuclear architecture as part of its replication process (Simpson-Holley, Colgrove et al. 2005). The nuclear membrane, in particular, becomes highly modified during the course of viral replication and is considered to be the primary site of envelopment for most herpes viruses (Darlington and Moss 1968; Schwartz and Roizman 1969).

High-resolution scanning and transmission electron microscopy proved some of the distortions of the nuclear surface in the course of viral multiplication to be related to enlargement of nuclear pores through which nuclear content and capsids protrude into the cytoplasm suggesting that capsids use impaired nuclear pores as gateways to gain direct access to the cytoplasm (Wild, Engels et al. 2005). Cells infected with alpha herpes viruses, such as HSV-1 or bovine herpes virus 1 (BoHV-1) disintegrate in the course of virus multiplication. This most likely involves fast disintegrating processes. The rapidity of cell disintegration suggests dramatic distortions within the nucleus and/or at the nuclear envelope. Such fast events can be recognized only by electron microscopy provided that the temporal resolution of the preparation methods applied is sufficient. In addition, structures must be kept in place during the follow-up preparation.

For many years, the advantages of surface imaging at the subcellular level were not available to the cell biologist, largely due to insufficient resolution of the scanning electron microscopes (SEM) employed. This situation was considerably improved by the introduction of field emission sources for SEMs, which were approximately 1000 times brighter than conventional sources, and facilitated surface imaging at much the same effective resolution for biological material as conventional transmission electron microscopy (TEM) (Allen 1993). Specified resolution for field emission instruments is around 1 nm, and it seems highly likely that the technology of biological specimen preparation is the major limiting factor at the moment (Allen, Rutherford et al. 1998).

In order to obtain a more detailed view onto the nuclear surface in HSV-1 infected cells we employed *in situ* preparation techniques at ambient temperatures, as well as cryo-preparation techniques of cell suspensions. Determination of the area between nuclear pores revealed that a single virion requires ten times more membranes for budding at the inner nuclear membrane than available at the nuclear envelope between nuclear pores of uninfected or of mock infected cells. In HSV-1 infected cells, the number of nuclear pores is substantially reduced. In addition, the diameter of both the pore channel and the entire pore complex becomes markedly enlarged. Transmission electron microscopy on cells prepared *in situ* confirmed impairment of the nuclear envelope at sites of nuclear pores, and furthermore, suggests that impaired nuclear pores are the gateway for capsid to exit the nucleus. Interestingly, nuclear pore proteins did not disappear from the nuclear surface but rather formed small aggregates that are irregularly distributed at the nuclear periphery.

# 3. MATERIAL AND METHODS

## 3.1 Viruses and Cells

Vero and HeLa cells were grown in Dulbecco's modified minimal essential medium (DMEM; Invitrogen, Basel, Switzerland) supplemented with penicillin (100 U/ml), streptomycin (100 g/ml) and 10% fetal calf serum (FCS; Omnilab, Mettmenstetten, Switzerland) for 2 days on cover slips for field emission scanning electron microscopy (FESEM), or on 30 μm thick sapphire disks covered with 8-10 nm carbon with a diameter of 3 mm for low temperature transmission electron microscopy (LTEM), or in cell culture flasks for cryo-FESEM and for polyacrylamide gel electrophoresis. Then cells were infected with herpes simplex virus 1-mono red fluorescence protein (HSV-1-VP26-mRFP) or wild-type herpes simplex virus type 1 (HSV-1-wt), provided by Claudia Senn, at a multiplicity of infection (MOI) of 2 or 5 and incubated at 37 °C for up to 24 h.

## 3.2 Field Emission Scanning Electron Microscopy

In order to examine the nuclear surface a methodology for *in situ* preparation of nuclei developed by T.Allen and coworkers (Allen, Rutherford et al. 1998) was applied as following. HeLa cells were grown on glass cover slips for 2 days. They were infected with HSV-1 at a MOI of 5 and incubated at 37 °C for up to 24 h. Then cells were fixed with 1% formaldehyde + 0.025% glutaraldehyde in 0.1 M Na/K-phosphate, pH 7.4, at room temperature for 1 minute, and permeabilized with 0.5% Triton-X-100 for 5 minutes. After postfixation with 1% osmium tetroxide at 4 °C for 30 minutes, cells were treated with 1% aequous thiocarbohydrazide at room temperature for 30 minutes. Then, a second time with 1% osmium tetroxide at room temperature for 30 minutes. Cells were dehydrated with a graded serie of ethanol starting at 70%, and critical point dried (BAL-TEC, CPD 030, Blazers, Liechtenstein). The dry samples were fractured

in this way. The glass cover slip with the dry cells on it was laid on an adhesive film on an electron microscope sample holder. This was firmly touched with another adhesive sample holder and pulled away without sideways movement (Fig. 3). Both the surface on which the cells were grown and the adhesive surface were shadowed with 5 nm platinum by sputter coating (BAL-TEC SCD500 High Vacuum Sputtering Device, Blazers, Liechtenstein). The coated samples were examined in a field emission scanning electron microscope (Gemini, Zeiss Supra 50 VP, Oberkochen, Germany) at an acceleration voltage between 5 and 20 kV using secondary electron signal.

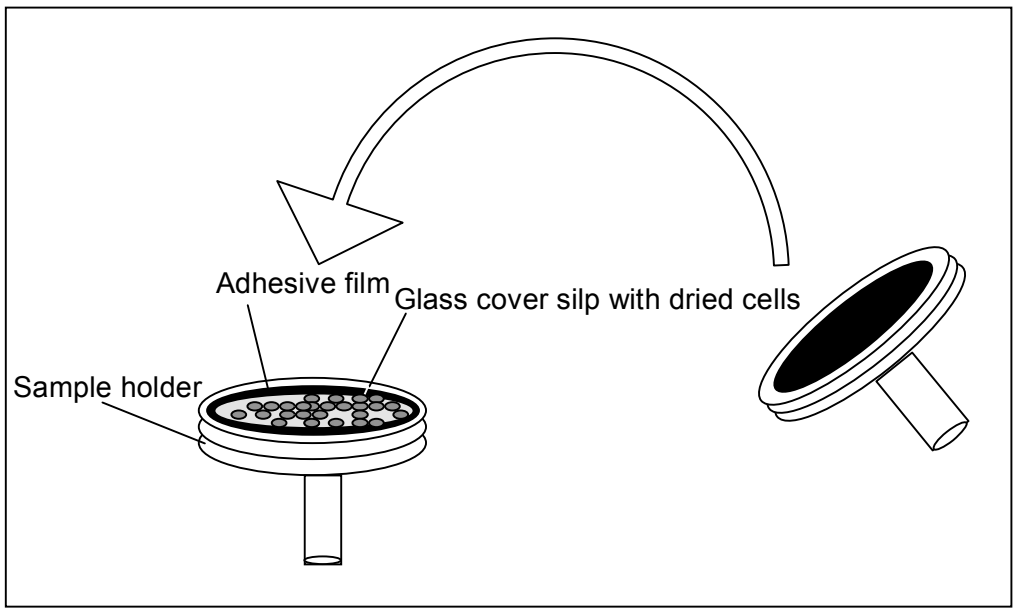


**Fig. 3.** Schematic drawing of sample fracturing.

**Determination of the nuclear surface area**

To estimate the amount of membranes available for budding of capsids at the nuclear envelope, the nuclear surface of mock infected HeLa cells was divided into triangles with a pore at each angle (see Fig. 14). The surface of triangles was calculated using the formula *b h /2*.

**Calculation of virial surface area**

Herpesviruses are spherical particles with a diameter of approximately 200 nm (Grunewald, Desai et al. 2003). In order to define the membrane surface required for the envelopment of a single virion of a final size of 200 nm in diameter by budding at the nuclear membrane, the surface area was calculated assuming HSV-1 virions are true spheres:

$$Surface\ of\ a\ sphere = \Pi\, d^2 = \Pi\, 200^2 \approx 125'000\ nm^2$$

### 3.3 Cryo-Field Emission Scanning Electron Microscopy

HSV-1 infected (MOI 5) and mock infected Vero cells grown in cell culture flasks were trypsinised and centrifuged at 1000 rcf. The pellet was resuspended in fresh medium and collected in microtubes. After fixation in 0.1-0.5% glutaraldehyde for 30 minutes aliquots were transferred into hexadecane (Studer, Michel et al. 1989) prior to sandwiching them between two aluminium platelets using a copper grid (100 mesh/inch) as a spacer. The sandwich of two flat aluminium specimen carriers coated with 20 nm of copper to render the surface hydrophilic was then placed in the holder of the high-pressure freezer HPM010 freezer (BAL-TEC inc., Blazers, Liechtenstein) for immediate freezing. The sandwich with the cells between the aluminium platelets was clamped in a special holder (Walther 1997) and cryo-fractured in a freeze-etching machine (BAF 300, BAL-TEC, Blazers, Liechtenstein) by removing one aluminium platelet with the microtome (temperature -110 °C, vacuum about 2 x $10^{-7}$ mbar). After 2 minutes of "etching" (sublimation of some water at the fracture face) the sample was double layer coated (Walther 1995) by electron beam evaporation with 5 nm of platinum-carbon at an angle of 45 °C and about 3-8 nm of carbon, perpendicularly. The sample was then mounted on a cryo-holder and transferred into the microscope (Gemini, Zeiss Supra 50 VP, Oberkochen, Germany) for analyzing the fracture surface of cells at a temperature of -130 °C and an

acceleration voltage of 10 to 20 kV. Micrographs were recorded digitally using the secondary electron signal in lens. Freezing, freeze-fracturing and cryo-FESEM were done at the Center of Electronmicrosopy, Swiss Federal School of Technology, Zurich.

### 3.4 Low Temperature Transmission Electron Microscopy

Vero and HeLa cells grown on sapphire disks, infected with HSV-1 (MOI 5) and incubated at 37 °C for 10 hours were frozen in a high-pressure unit (HPM010, BAL-TEC Inc., Blazers, Liechtenstein). Frozen cells were transferred into a freeze-substitution unit (FS 7500, Boeckeler Instruments, Tucson, Arizona, USA) precooled to -88 °C for substitution with acetone and subsequent fixation with 0.25% glutaraldehyde and 0.5% osmium tetroxide at temperatures between -30 °C and +2 °C as described in detail (Wild, Schraner et al. 2001) and embedded in Epon. 50 to 60 nm thick sections were analyzed in a TEM (CM12, Philips, Endhoven, The Netherlands) equipped with a slow scan CCD camera (Gatan, Pleasanton, California, USA) at an acceleration voltage of 100 kV.

### 3.5 Confocal Microscopy

HeLa cells were grown for 2 days on cover slips of 10 mm in diameter (Mattek, Ashland, MA, USA). Then cells were infected with HSV-1-VP26-mRFP or with HSV-1-wt at a MOI of 5 and incubated at 37 °C for 6, 8, 10, 12, 14, 18h. After fixation with 2% formaldehyd for 25 minutes at room temperature, the cells were permeabilized with 0.1% Triton-X-100 at room temperature for 7 minutes. To identify nuclear pores, immunolabeling of the HSV-1-VP26-mRFP infected cells was done using monoclonal antibodies against nuclear pore proteins p62, p152, p90 (Mab414, Covance, Berkeley California, USA) at a dilution of 1:1’000. After three washes with phosphate-buffered saline (PBS) + 0.05% Tween 20, cells were incubated with 1:500 dilution of Alexa488 (Molecular Probes, Eugene, Oregon, USA) secondary antibodies (anti-mouse).

Ascertainment of infectivity was done with antibodies against VP22 or VP16 (kindly provided by B. Roizman) with 1:1'000 dilution and secondary antibodies Alexa594 (Molecular Probes, Oregon, USA). Alternatively, a virus expressing red fluorescent protein (HSV-1-VP26-mRFP) was used. Samples were embedded in fluorescence mounting medium (DakoCytomation, Glostrup, Denmark) and analysed using a confocal laser scanning microscope (SP2, Leica, Mannheim, Germany). Images were deconvolved employing a blind deconvolution algorithm using the program suite Huygens Essential (SVI, Hilversum, The Netherlands). Confocal microscopy was performed at the Institute of Parasitology and the Institute of Anatomy, University of Zurich.

### 3.6 Polyacrylamide Gel Electrophoresis and Immunoblotting

HeLa cells were grown in 25 $cm^2$ cell culture flasks. Cells were infected with HSV-1 at a MOI of 2 and incubated at 37 °C for 0, 8, 10, 12, 24 h. The protein extraction was accomplished as following. After washing with PBS, the cells were detached with trypsin and centrifuged by 800 g for 2 minutes. The cell pellets were resuspended in Ripa Buffer (50 mM Tris-HCl pH 7.4, 150 mM NaCl, 1 mM PMSF, 1 mM EDTA, 1% Triton-X-100, 1% Na-deoxycholate, 1 µg/ml Aprotinin and 1 mg/ml Leupeptin, 0.1% SDS) for 20 minutes on ice and centrifuged by 10'000 g for 5 minutes at 4 °C. The supernatant was transferred in new Eppendorf tubes and the protein concentration was determined based on the method of Bradford. After adding of protein lysis buffer (0.5 M Tris-HCl pH 6.8, 4.4% SDS, 1% β-mercaptoethanol, 20% glycerol, 1% brom phenol blue, $H_2O$), the samples were boiled for 5 minutes. 10 µg protein of each sample were separated on 6% SDS-polyacrylamid gel. After electrophoresis at 100 V for 2 h, the gel was transferred to a polyvinylidene difluoride membrane. Blots were blocked with 5% low-fat milk in H-PBST (50 mM sodium phosphate buffer containing 155 mM NaCl, 0.05% Tween 20 and 10 mM HEPES) over night. Subsequently, blots were probed with a 1:5'000 dilution of Mab414 (Covance,

Berkeley California, USA) with H-PBST. After two washing steps with H-PBST, blots were incubated with 1:30’000 dilution of HRP-conjugated anti-mouse secondary antibodies (Sigma-Aldrich, Switzerland). Blots were visualized on X-ray film using chemiluminescence.

# 4. RESULTS

## 4.1 Nuclear Pores dilate and Pore Number reduces

NPCs form a key transport barrier between the cytoplasm and the nucleus. In non-dividing cells, nucleocytoplasmic shuttling of macromolecules is tightly controlled by their selective translocation through the 30 to 50 nm long (Stoffler, Fahrenkrog et al. 1999) and 9 nm wide (Pante and Aebi 1993) NPC central channel. This channel was shown to be expandable, enabling the transport of macromolecules with diameters of up to ~39 nm (Pante and Kann 2002). (Goldberg, Wiese et al. 1997) found that "holes" or pores with a diameter of 35 to 45 nm were relatively abundant. Pores may exhibit a distinctly non-random distribution over the nuclear surface. However, there appears to be a minimum interpore distance that influences their distribution on the nuclear envelope (Maul 1971). In some cells nuclear pores occur in regular geometric arrays (Franke 1974). The density of pores per unit area of the nuclear envelope varies considerably among different cell types (Maul 1977). A general value for differentiated higher eukaryotic cells is 10 to 20 pores/1 $\mu m^2$ (yielding a total of 2000-4000 pores/nucleus).

Nuclear pores have been shown to become impaired in the course of bovine herpes virus multiplication while nuclear membranes seem to remain morphologically intact (Wild, Engels et al. 2005). Distortion of nuclear pores was, hence, assumed to function as gateways for capsids to pass the nucleocytoplasmic barrier rather than to play an essential role in cell disintegration.

In order to clarify whether there are similar morphological phenomena at the nuclear surface in the course of HSV-1 infection, HeLa cells have been investigated applying 3 different methods. First, confluently grown HeLa cells

on cover slips were infected with HSV-1. After fixation, permeabilisation, postfixation, critical point drying, fracturing and shadowing with platinum, the samples were examined in a field emission scanning microscope. FESEM revealed distinct morphological changes of the NPCs. The NPC central channel was dilated between 100 to 133 nm in HSV-1 infected cells (Fig. 5D and E). The NPCs diameter was up to 290 nm wide.

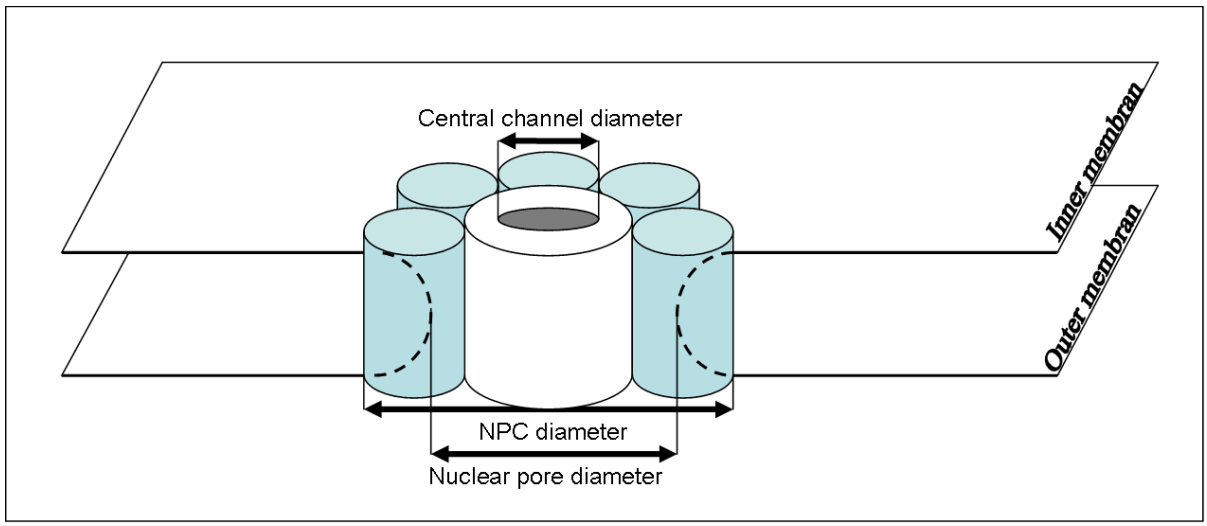


**Fig. 4.** Schematic drawing of a nuclear pore complex showing the diameters.

The central channel diameter in mock infected cells was in average 20 nm (Fig. 5C). The distribution of NPCs on the nuclear envelope showed a regular dissemination of the pores in mock infected cells (Fig. 5A). In infected cells, the NPCs grouped in some areas so that they were irregularly disseminated on the nuclear envelope. Many of them were plumper and stood more out of the nuclear membrane. The interpore distance has been observed to be larger in infected cells than in mock infected cells (Fig. 5B). Therefore, the nuclear pores were counted on randomly selected areas. In average, 29.07 NPC/1 $\mu m^2$ have been counted on mock infected nuclei. In HSV-1 infected nuclei, the number of NPCs per 1$\mu m^2$ was considerably reduced averaging 6.47 NPC/1 $\mu m^2$ (Table I).

| Cells | NPC/$\mu m^2$ | Cells | NPC/$\mu m^2$ |
|---|---|---|---|
| HSV 15h | 7.00 | Mock0 | 28.00 |
| HSV 15h | 5.60 | Mock1 | 27.80 |
| HSV 15h | 8.75 | Mock2 | 21.70 |
| HSV 15h | 5.30 | Mock3 | 31.30 |
| HSV 15h | 7.20 | Mock4 | 34.30 |
| HSV 15h | 4.83 | Mock5 | 36.40 |
| HSV 15h | 6.60 | Mock6 | 24.00 |
| Mean | 6.47 | Mean | 29.07 |
| SD | 0.5081 | SD | 2.005 |

**Table I.** Number of NPCs on FESEM images of HSV-1 infected and mock infected HeLa cells incubated for 15 h. The means were statistically different ($p<0.0001$) as compared by a students T-test.

Budding of capsids requires large amount of membranes. In order to clarify whether enough membranes are available between pores for capsids to bud, the nuclear surface was divided into triangles with a pore at each angle. In average, an area of 11'300 $nm^2$ was calculated per triangle. The surface area of the envelope of a single virion was calculated assuming the virion to be a sphere with a diameter of 200 nm giving 125'000 $nm^2$. To our surprise, the membrane area between 3 pores is ten times smaller than that required for budding of a single capsid.

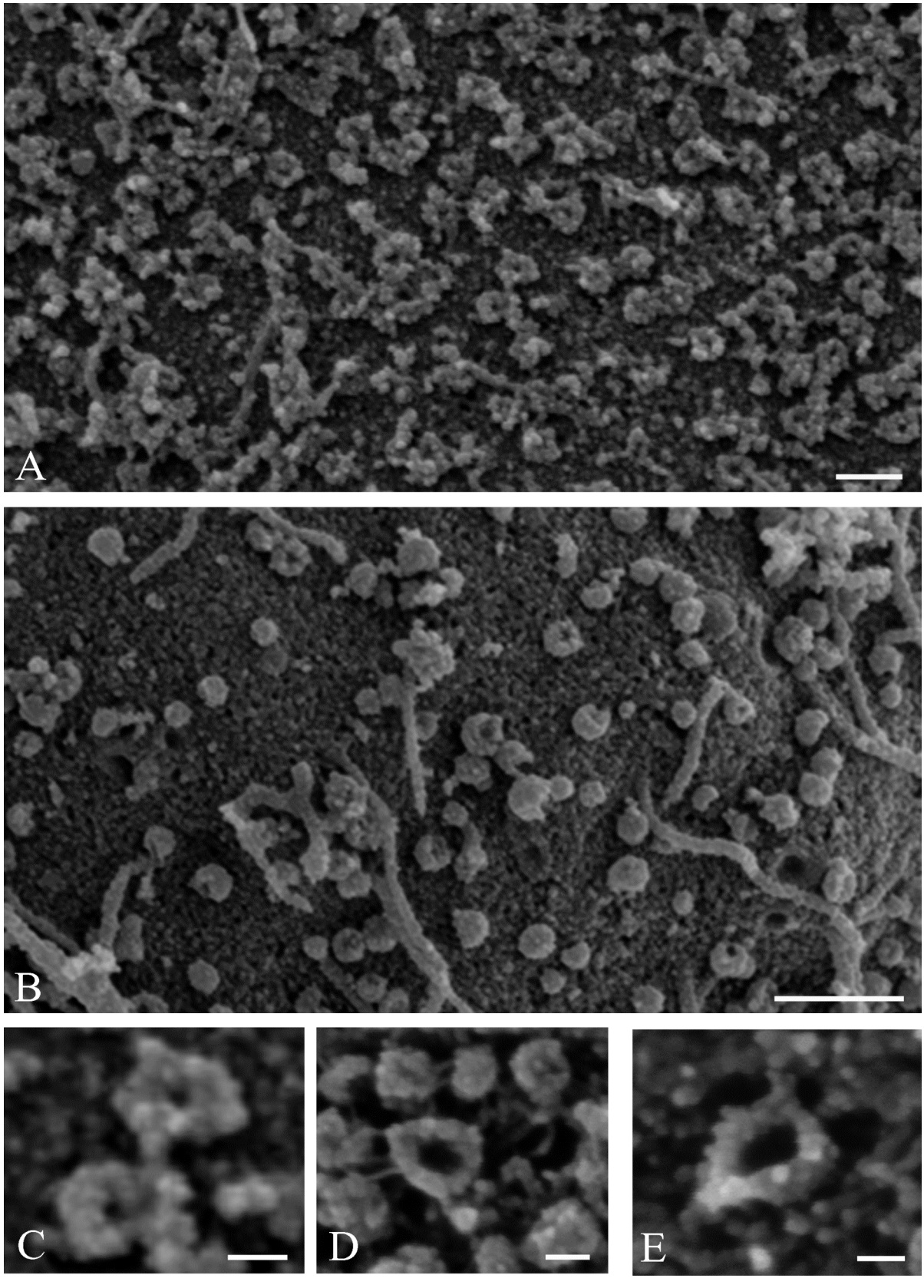


**Fig. 5.** *In situ* access to nuclei of HeLa cells. FESEM images of the nuclear surface of mock infected (A) and HSV-1 infected HeLa cells 18 h post infection (p.i.) (B). Central channel diameter in mock infected cells (C) is 20 nm and in HSV-1 infected cells dilated to 113 nm (D) or 124 nm (E). Bars, 200 nm (A), 500 nm (B), 100 nm (C-E).

### 4.2 Nuclear Surface protrudes into the Cytoplasm

To verify the changes found on the nuclear envelope in HeLa cells after infection with HSV-1, cryo-FESEM was performed. Vero cells grown in culture cell flasks were collected after trypsinisation, frozen, freeze-etched and transferred into the microscope. This technique permits the observation of fractured inner and outer nuclear envelope faces as well as their profiles.

Nuclear pore diameters were observed to be dilated up to 570 nm in HSV-1 infected cells (Fig. 6A and C). The nuclear envelope presented protrusions with intact nuclear membranes with diameters at the base of up to 2.8 μm. On the surface of these protrusions no NPC has been found (Fig. 7A). Nuclear envelopes were locally folded (Fig. 6B). In mock infected cells, the nuclear envelope presented no protrusions or folds (Fig. 7B). The size of nuclear pores was between 65 nm and 125 nm (Fig. 6D). The large differences are probably related to the fracture plane.

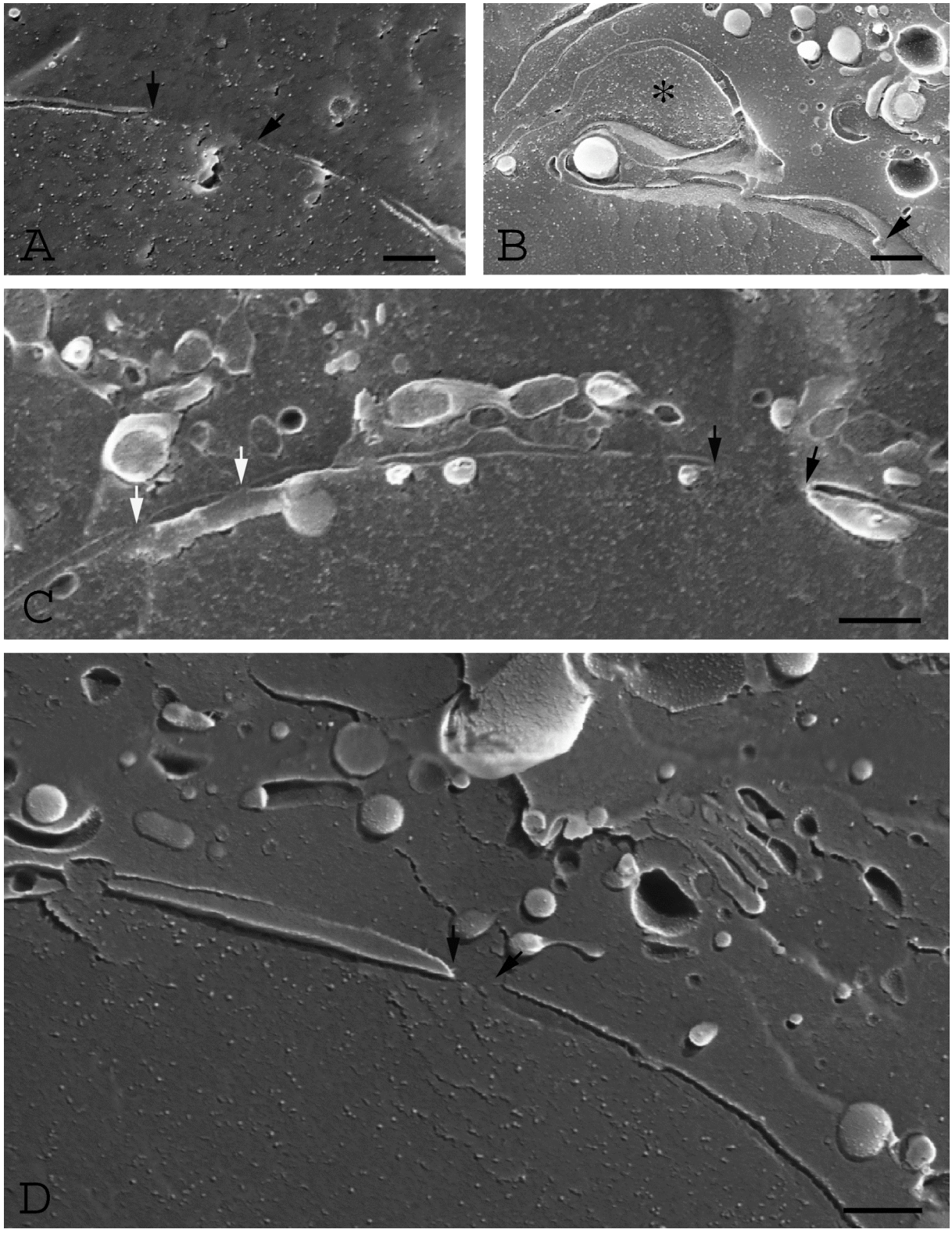


**Fig. 6.** Cryo-FESEM images of HSV-1 (A-C) and mock (D) HeLa cells 17 h p.i. after freezing, freeze-fracture, freeze-etching and platinum shadowing. The pore diameters in HSV-1 infected cells are dilated to 420 nm (black arrows, A) and 570 nm (black arrows, C). The nuclear membrane is folded (*, B). Local fusion between inner and outer nuclear membrane creating the nuclear pore (arrow, B). Normal pore diameter of 65 nm (arrows, D), 105 and 125 nm (white arrows, C). Bars, 200 nm (A, D); 500 nm (B, C).

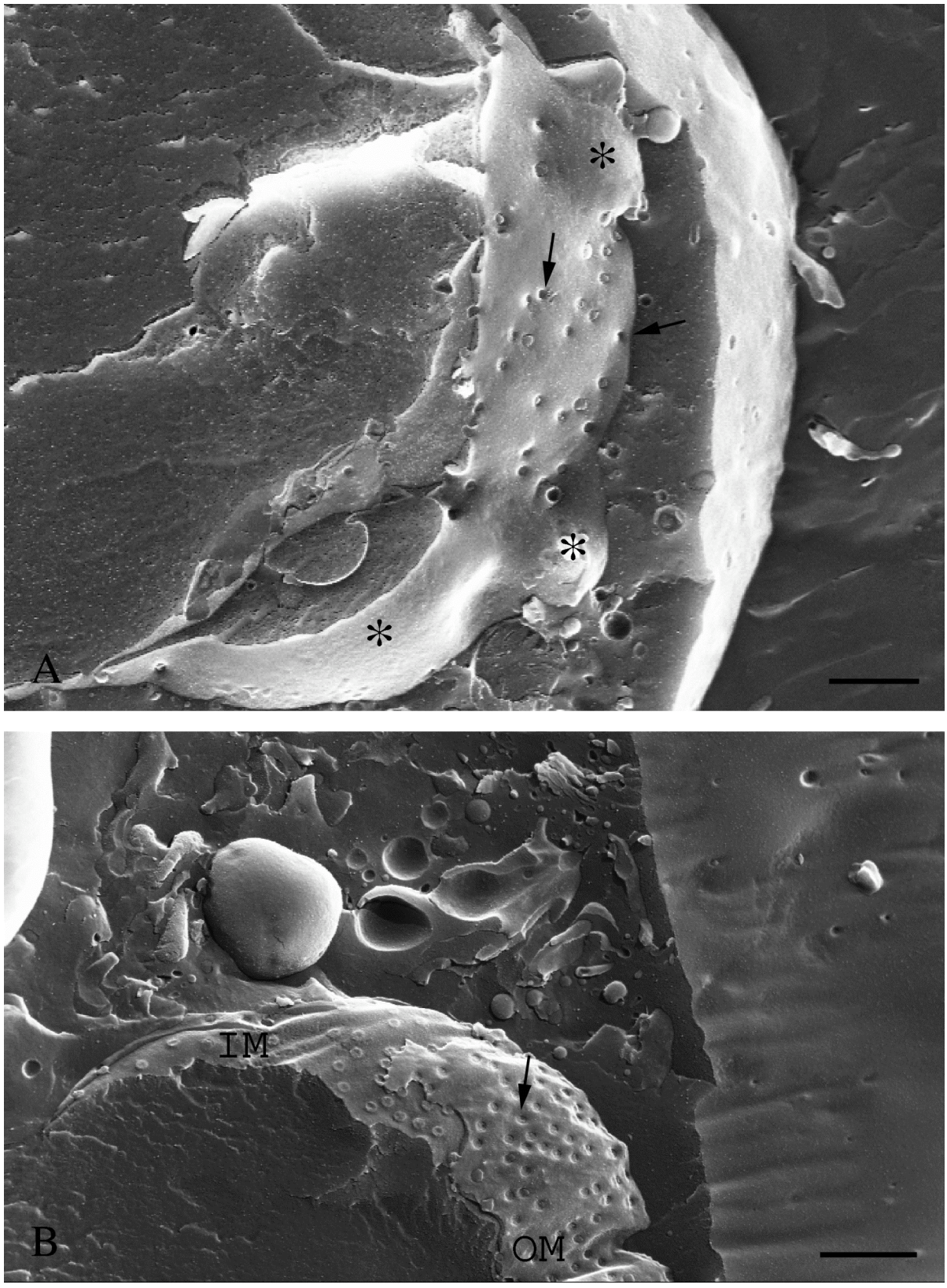


**Fig. 7.** Cryo-FESEM images of HSV-1 (A) and mock (B) HeLa cells 17 h p.i. after freezing, freeze-fracture, freeze-etching and platinum shadowing. Protrusions without pores of the nuclear surface (*, A). Normal nuclear envelope of a mock infected cell with nuclear pores (B, arrow). IM= inner nuclear membrane; OM=outer nuclear membrane. Bars, 1 μm.

### 4.3 Low Temperature Transmission Electron Microscopy

In order to analyse the nuclear envelope, we investigated Vero cells infected with HSV-1 for 10 hours by LTEM to get an idea about the effect of the virus multiplication on the nuclear pores. Vero cells grown on sapphire disks were frozen, freeze-substituted and embedded in Epon. Sections were analyzed in a TEM.

The nuclear matrix protruded into the cytoplasm through nuclear pores, which were dilated up to 650 nm (Fig. 8A and C). The protruding nuclear matrix often contained capsids (Fig. 8C). Dilated nuclear pores were clearly bordered at least at one side with the inner nuclear membrane continuing into the outer nuclear membrane (Fig. 8A). Nuclei of infected cells exhibited also intact 100 to 110 nm wide nuclear pores (Fig. 8B) with a distinct central layer corresponding to the central ring and a cloudy layer corresponding to the cytoplasmic ring and filaments of the nuclear pore complex (Pante 1996). The diameter of isolated non-infected nuclear pore complexes is 125 nm (Pante 1996). Wild, Engels et al. (2005) measured diameters of intact pores of 100 to 120 nm in thin sections. The discrepancy in pore diameters is probably due to section thickness that does not allow precise measurements.

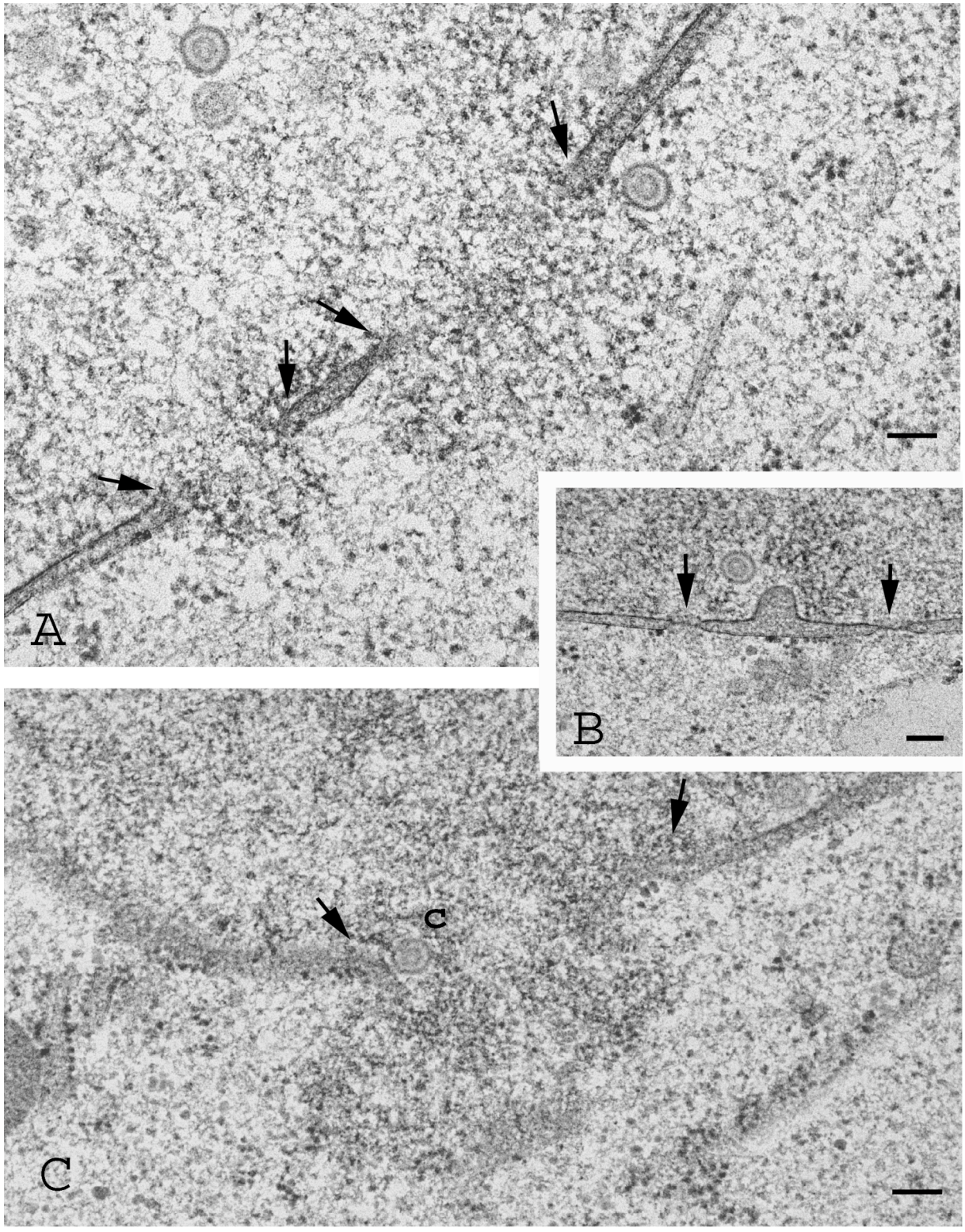


**Fig. 8.** Sections through Vero cells infected with HSV-1 at a MOI of 5 for 10 hours. Distinctly defined nuclear pores that are dilated to 280 and 520 nm (arrows, A). Intact nuclear pores of 100 nm (arrows, B). Protrusion of nuclear matrix containing a capsid (c) into the cytoplasmic matrix (arrows, C). Whether or not the gap in the nuclear envelope is a dilated nuclear pore cannot be verified. Bars, 100nm.

### 4.4 Nuclear Pore Proteins are irregularly distributed

Electron microscopy provides clear evidence for dramatic structural alterations of nuclear pores suggesting that they may function as gateways for capsids to exit from the nucleoplasm to the cytoplasmic compartment. Nuclear pore impairments may correlate with the degradation of certain nuclear pore proteins e.g. Nup153, p62 as in cells infected with poliovirus (Gustin and Sarnow 2001; Gustin and Sarnow 2002). In order to determine possible changes in distribution of nuclear pore proteins in HSV-1 infected cells, cells were immunolabeled using antibodies against p62, p152, p90 (Mab414). To ascertain the state of infection, cells were infected with virus expressing red fluorescence protein (HSV-1-VP26-mRFP). Alternatively, HSV-1-wt infected cells were monitored by immunolabeling using antibodies against tegument protein VP22 or VP16. Samples were analysed using a confocal laser scanning microscope.

First changes became obvious as early as 6 h p.i. In HSV-1-VP26-mRFP and HSV-1-wt infected cells, labeled nuclear pore proteins built clusters containing probably grouped NPCs (Fig. 9A-D). Mock infected cells exhibits regularly disseminated nuclear pore proteins (Fig. 9E and F) at all infection times. In HSV-1 infected cells, labeling with Mab414 revealed also clusters of pore proteins on the nuclear surface (Fig. 10A and B). Labeling of mock infected cells was similar as described above. The signal showed a small punctuated pattern of NPCs (Fig. 10C and D). The punctuate pattern can be resolved into single NPCs, at least under carefully controlled and favourable conditions because the resolution of the confocal microscope is sufficient to visualize single NPC-sized particles and to distinguish between single particles and particle aggregates (Kubitscheck and Peters 1998). The intensity of fluorescence signals seemed to be increased in HSV-1 and HSV-1-VP26-mRFP infected cells compared to mock infected cells.

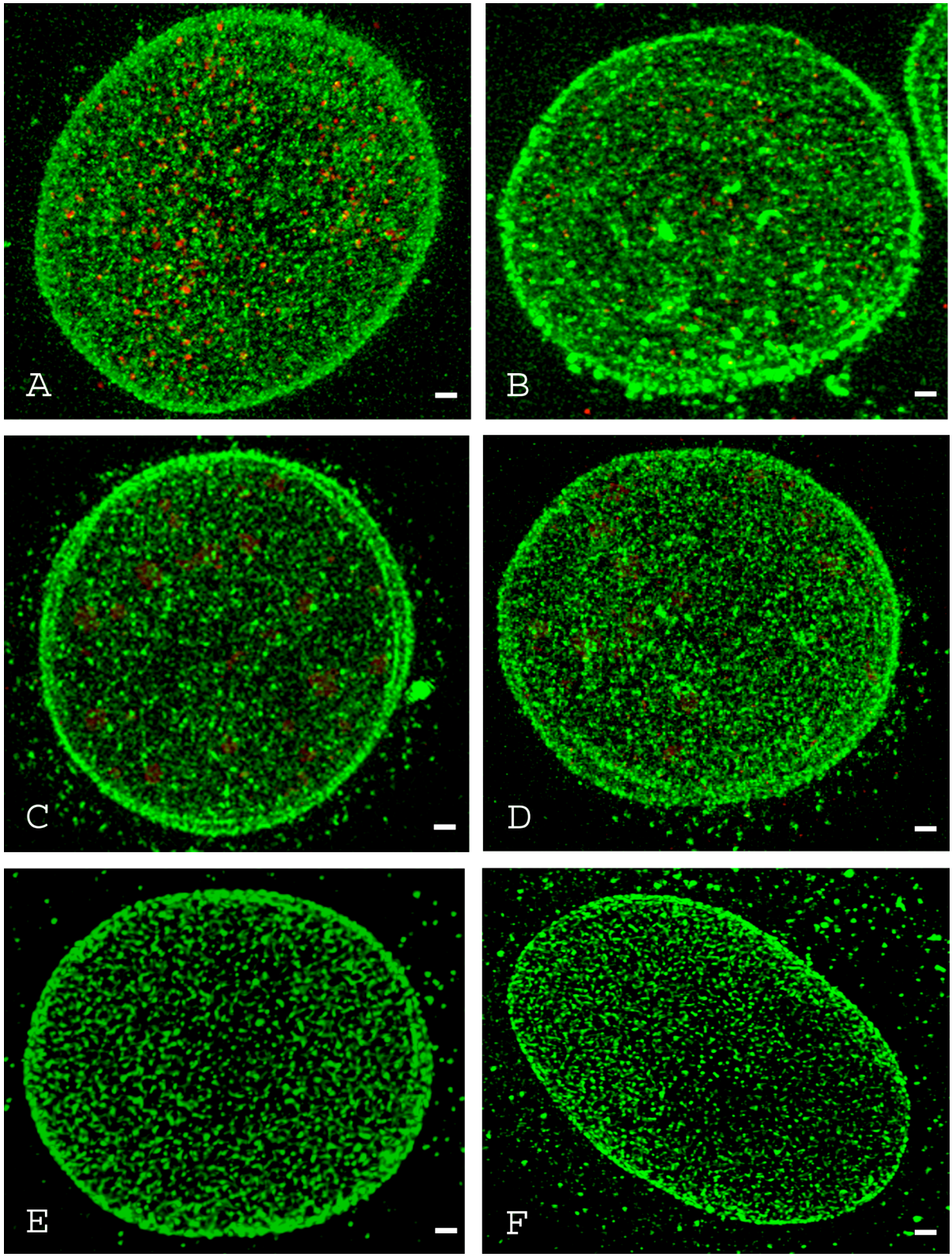


**Fig. 9.** HeLa cells infected with HSV-1-VP26-mRFP (A-D) and mock infected cells (E, F). Cells were incubated for 6 h (A), 8 h (B), 10 h (C) 12 h (D, E) or 14 h (F) and immunolabeled with Mab414. In HSV-1-VP26-mRFP infected HeLa cells (A-D), fluorescence signal is irregular forming small clusters whereas in mock infected cells it is regularly disseminated on the entire nuclear envelope (E, F). Bars, 1µm.

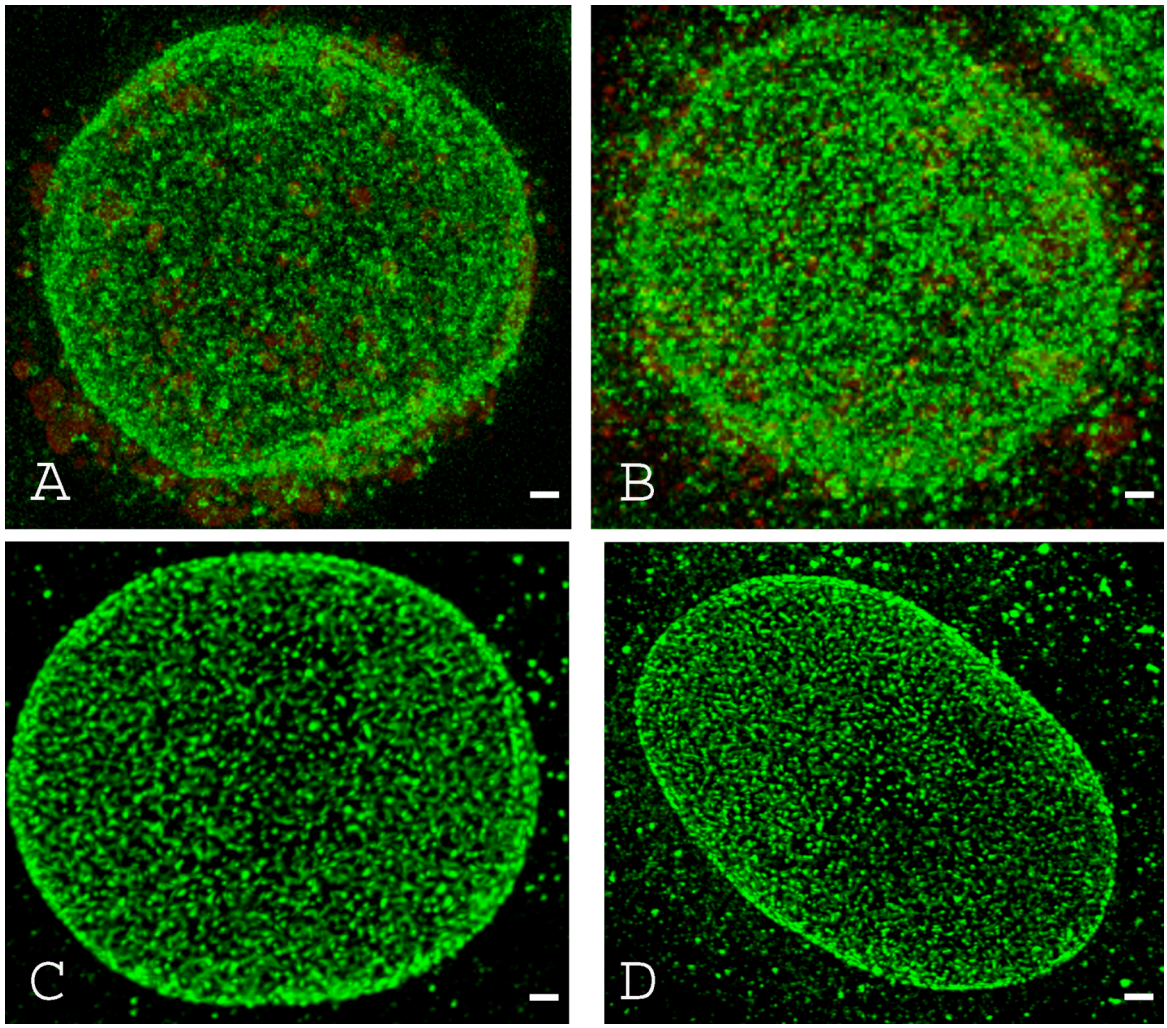


**Fig. 10.** HeLa cells infected with HSV-1-wt (A, B) or mock infected (C, D). Cells were incubated for 12 h (A, C) or 14 h (B, D) and immunolabeled with Mab414 and VP22. In HSV-1 infected HeLa cells (A, B), fluorescence signal is irregular forming small clusters whereas in mock infected cells it is regularly disseminated on the entire nuclear envelope (C, D). Bars, 1µm.

To verify whether changes in nuclear pore protein distribution in HSV-1-VP26-mRFP infected cells was not due to insertion of mRFP, infectivity was ascertained by immunolabeling using antibodies against tegument proteins VP16 and VP22. As shown in Fig. 10, distribution of nuclear pore proteins was the same as in HSV-1-VP26-mRFP infected cells.

### 4.5 Nuclear Pore Proteins Quantification

While analysing confocal microscopic images, the impression arose that in infected cells Mab414 fluorescence signals is increased compared to mock infected cells. To clarify whether the increment of fluorescence signal was due to an increase in number of NPCs, nuclear pore proteins were analysed by Western blots using Mab414 as primary antibodies and HRP-conjugated secondary antibodies. The results obtained in HSV-1 infected cells at any time of incubation were similar to those in mock infected cells (Fig. 11).

These data suggest that the increment (if any) in fluorescent signals is due to breakdown of NPCs giving better access to antibodies, than due to increment of pore proteins.

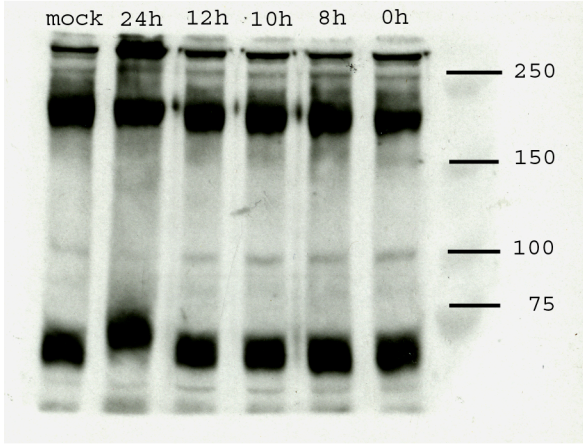


**Fig. 11.** Western blot analysis of nuclear pore proteins of mock infected and HSV-1 infected HeLa cells. No obvious changes of nuclear pore proteins were observed between mock infected and HSV-1 infected samples.

### 4.6 Localization of VP22 and VP16 in HSV-1 infected Cells

Further observations have been made according to the localization of VP22 and VP16. HeLa cells were infected with HSV-1-wt, fixed and stained for VP16 and VP22 antibodies. From 10 h p.i. on both virus proteins were detectable, largely spread through the cytoplasm and the nucleus. At 14 h p.i., VP22 was in the nucleus, mainly situated at the nuclear periphery (Fig. 12A). VP16 built clusters located obviously in the cytoplasm. Fewer fluorescence signal of VP16 was detected in the nucleus at this time. (Fig. 12B). The three dimensional reconstitution (Fig. 13) shows also the localization of both tegument proteins in the nucleus and at its periphery.

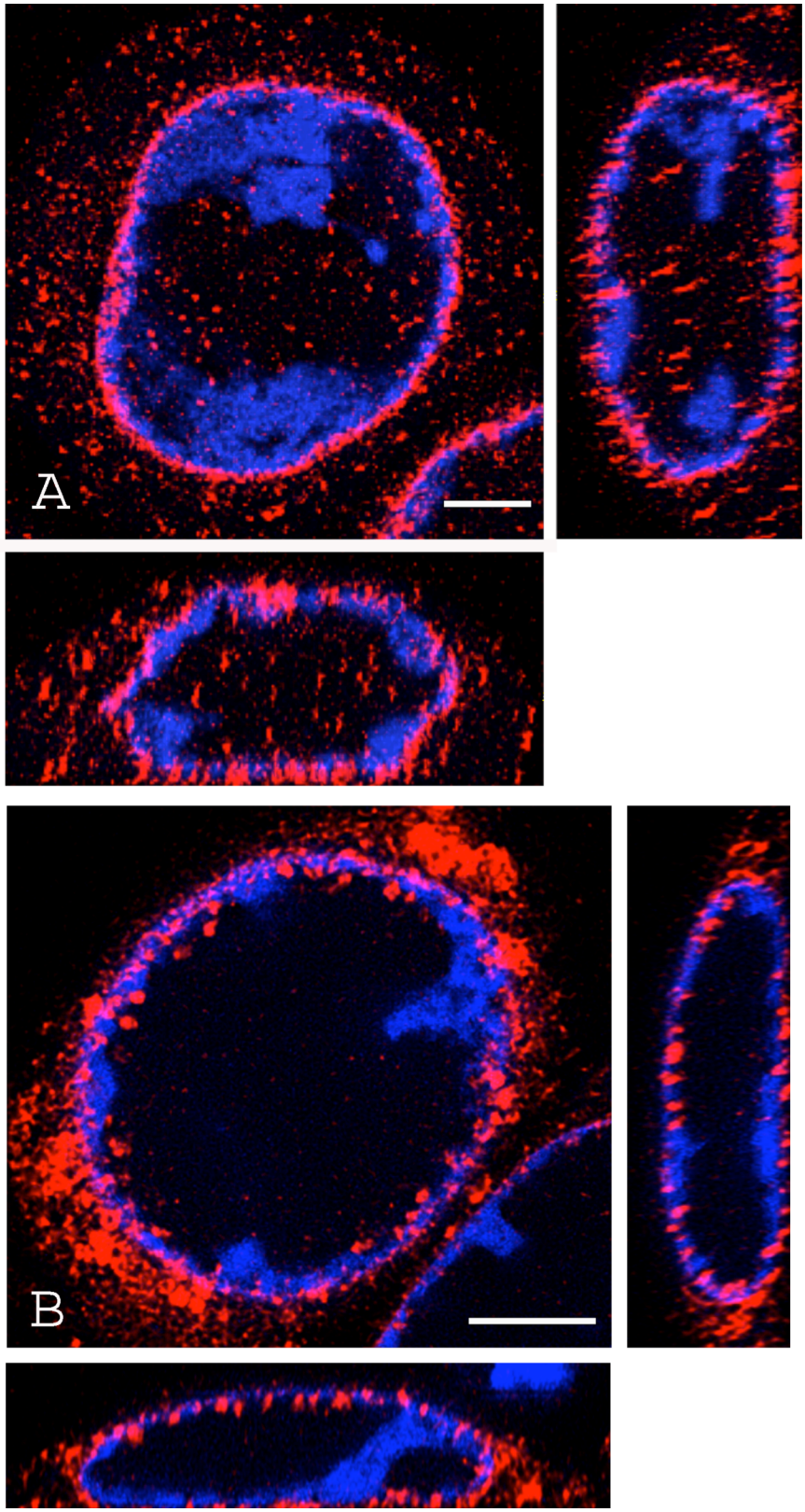


**Fig. 12.** Confocal micrographs of HSV-1 infected HeLa cells 14 h p.i. incubated with antibodies against VP22 (A) respectively VP16 (B). Both VP16 and VP22 are located within the cytoplasm and within the nucleus but mainly at the nuclear periphery. Bars, 3 µm (A), 5 µm (B).

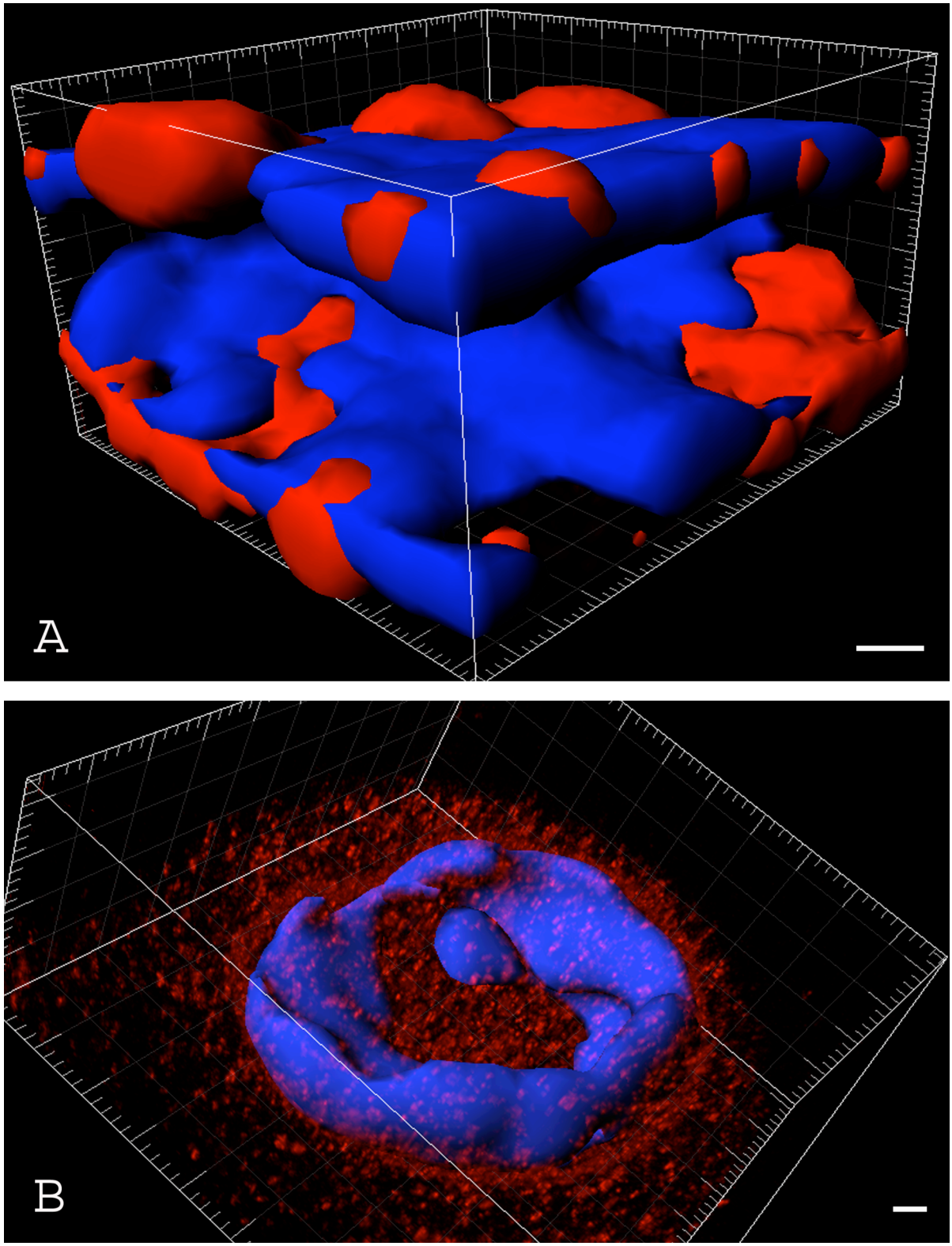


**Fig. 13.** Three dimensional reconstitution of HSV-1 infected HeLa cells 14 h p.i. (A) incubation with antibodies against VP16 and (B) against VP22 at a dilution of 1:1'000. Both virus proteins are located in the nucleus and the cytoplasm. Bars, 1 µm.

# 5. DISCUSSION

Membranes of cells productively infected with herpes viruses undergo distinct morphological, biochemical, and immunological changes as viral replication proceeds from the early stages of infection to the production of new virions and eventual host cell destruction (Haines and Baerwald 1976). The nuclear membrane, in particular, becomes highly modified during the course of viral replication and is considered to be the primary site of envelopment for most herpes viruses (Darlington and Moss 1968; Schwartz and Roizman 1969). The capsid acquires envelope and tegument proteins by budding through the inner nuclear membrane resulting in a fully enveloped virion within the perinuclear space (Roizman 2001). The pathway for capsids through the nucleocytoplasmic barrier and the acquisition of tegument and envelope are yet not fully understood (Homman-Loudiyi, Hultenby et al. 2003).

## 5.1 The Nuclear Envelope before the first Budding

Envelopment at the inner nuclear membrane requires large amount of membranes. The nuclear envelope is studded with nuclear pores. A general value of nuclear pores in differentiated higher eukaryotic cells is 10 to 20 pores/1 $\mu m^2$ (Maul 1977). In this study, the nuclear pores were counted on randomly selected areas of the nuclear surface. In average, 29.07 NPC/1 $\mu m^2$ have been counted on mock infected nuclei. In HSV-1 infected nuclei, the number of NPCs per 1$\mu m^2$ was considerably reduced averaging 6.47 pores/1 $\mu m^2$ 15 h p.i. To estimate whether enough membranes are available between nuclear pores for budding of capsids early in infection, the nuclear surface was divided into triangles with one pore at each angle. In average, an area of 11'300 $nm^2$ was calculated per triangle. A single virion of a final size of 200 nm in diameter requires about 125'000 $nm^2$. Therefore, the membrane area between

pores is more than ten times smaller than the surface area of a single virion (Fig. 14).

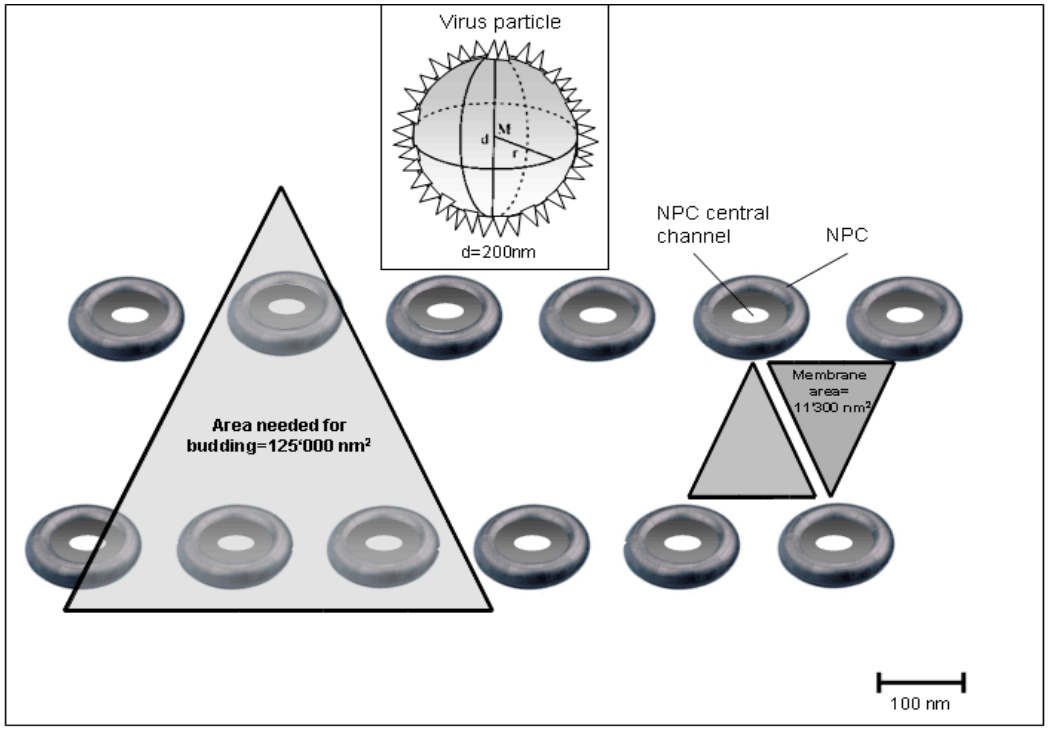


**Fig. 14.** Schematic drawing of size and distribution of NPCs. The nuclear surface was divided in small triangles with one pore at each angle. Small triangles represent the membrane area available between three pores. The big triangle shows the surface required for budding of one virion.

Consequently, capsids cannot bud at nuclear membranes unless the amount of membrane necessary for budding is provided. The question arises how will be the amount of membranes provided that is necessary for budding. One possibility is that NPCs disappear. The area one single pore occupies on the nuclear envelope is 12'500 $nm^2$. Ten pores have thus to disappear to provide the area a single capsid needs for budding. If this idea is true the disappearance of NPCs will need to be initiated by viral factors prior to the first budding which takes place at about 5 h after infection at MOI 5 (Cantieni 2000). Disappearance of NPCs, however, results in holes of the nuclear envelope which must be covered by the inner and outer nuclear membrane. Consequently, for each NPC that is removed the doubled area of membranes must be inserted to guarantee integrity of the nuclear envelope, i.e. the membrane area needed to substitute the

area of 10 pores equals 250'000 $nm^2$ of which 125'000 $nm^2$ can be used by a capsid for budding at the inner nuclear membrane. Therefore, loss of nuclear pores must be in concert with insertion of membrane constituents to provide the basis for successful budding. Indeed, it has been shown that [$^{32}$P]-phosphate was incorporated into nuclear membranes in the course of HSV-1 infection (Sutter 2006). This study did, however, not examine phospholipids metabolism early in infection prior to the first budding.

Enlargement of the area between nuclear pores can also be accomplished simply by insertion of membrane constituents. If membrane constituents are inserted in the already established nuclear membrane, it will result in an increase of the membrane area. The consequence is the formation of membrane folds by a constant nuclear volume. In the present study, folds of the nuclear envelopes have been locally found. To avoid folding of the nuclear membrane, the nuclear volume must increase. The nuclear size increases due to cellular mechanisms for the control of nuclear shape and size in uninfected cells (Simpson-Holley, Colgrove et al. 2005) and/or due to enlargement of extra-chromosomal compartments such as accumulation of capsid proteins VP26. Nuclear size has been reported to increase during HSV-1 infection (Monier, Armas et al. 2000; Simpson-Holley, Colgrove et al. 2005; Wild, Engels et al. 2005). This suggests that HSV-1 disrupts the mechanisms for the control of nuclear shape and size, allowing nuclear expansion outside normal cellular limits. Whether nuclear size increases early in infection needs to be proved.

In conclusion, virions need membrane already at the beginning of replication at an amount larger than that available on the surface of intact nuclei for successful budding. Thus, viral factors have to initiate the possibly disappearance of NPCs in concert with insertion of membrane constituents prior to budding.

### 5.2 The Nuclear Envelope during the Budding of hundredths of Capsids

The fate of virions derived by budding at the inner nuclear membrane is

controversially discussed. There are three theories for the escape of capsids out of the perinuclear space. 1. The fusion theory: The envelope derived by budding at the inner nuclear membrane fuses with the outer nuclear membrane (Gong and Kieff 1990; Whealy, Card et al. 1991; Card, Rinaman et al. 1993; Gershon, Sherman et al. 1994; Zhu, Gershon et al. 1995; Browne, Bell et al. 1996; Church and Wilson 1997; Granzow, Weiland et al. 1997; Klupp, Baumeister et al. 1998; Granzow, Klupp et al. 2001; Skepper, Whiteley et al. 2001). 2. The vesicle formation theory speculates that virions escape from the perinulcear space via vesicle formation at the outer nuclear membrane (Gershon, Cosio et al. 1973; Campadelli-Fiume, Farabegoli et al. 1991; Torrisi, Di Lazzaro et al. 1992; Radsak, Eickmann et al. 1996; Church and Wilson 1997; Granzow, Weiland et al. 1997). 3. The intraluminal transportation theory: Enveloped virions were found in the perinuclear space and rough endoplasmic reticulum (RER) (Schwartz and Roizman 1969; Whealy, Card et al. 1991; Gilbert, Ghosh et al. 1994; Radsak, Eickmann et al. 1996; Granzow, Weiland et al. 1997; Roller, Zhou et al. 2000; Wild, Engels et al. 2005). Connectivity from the perinuclear space to Golgi cisterns was discovered (Wild, Schraner et al. 2002) indicating that virions can be transported from the perinuclear space via RER cisternae into Golgi cisternae.

### 5.3 Nuclear Membranes are provided

Nuclear membranes of HSV-1 infected cells showed an increased level of [$^{32}$P]-phosphate incorporation compared to mock infected cells at 12 and 16 h p.i. (Sutter 2006). The differences of level of [$^{32}$P]-phosphate incorporation were between 23.7 to 52%. This result indicates that de novo synthesized phospholipids are inserted into nuclear membranes. If the theory of de-envelopment is correct no phospholipids will be lost at the nuclear membrane because membrane constituents inserted into the outer nuclear membrane need to recycle back to the inner nuclear membrane to avoid enlargement of the outer

nuclear membrane at infinity. Therefore, only a limited amount of phospholipids needs to be inserted into the nuclear membrane that must take place prior to the first budding. If the theory of intraluminal transportation is correct the membrane needed for budding at the inner nuclear membrane will be lost and thus must be replaced to maintain the nuclear envelope. If the vesicle formation theory is correct, more than the double amount of membranes will have to be replaced.

### 5.4 Loss of Nuclear Pores

The number of NPCs per 1 $\mu m^2$ was found to be five times lower in HSV-1 infected cells 15 h p.i. compared to mock infected cells. The nuclear envelope presented protrusions with intact nuclear membranes with diameters at the base of up to 2.8 μm. On the surface of these protrusions no NPCs has been found. The question arises whether this loss of NPCs is virus induced or due to mechanical stress because of the membrane dynamics in the course of budding of capsids. Considering the theory of de-envelopment, recycling of membrane constituents from the outer to the inner nuclear membrane would require movements of membranes in the area of the nuclear pores (Fig.15). This might result in instabilities at the structures of the NPC anchorage. Considering the theories of intraluminal transportation and vesicle formation, loss of membrane at the inner and outer nuclear membrane must be replace either by membrane constituents from other cellular sites or by de novo synthesis. The fact that [$^{32}$P]-phosphate is incorporated into nuclear membranes (Sutter 2006) implies that de novo synthesized phospholipids are incorporated into nuclear membranes. Insertion of de novo synthesized phospholipids might also lead to instabilities at the anchorage site of NPCs (Fig. 16). Another possibility for loss of NPCs is that a signal induction of viral proteins would induce functional disorders of NPC anchorage proteins like gp210 and Nup153 (Fig. 1). Glycoprotein gp210 is a membrane protein to which NPCs are anchored. It has been estimated to be

present in 16 to 24 copies per nuclear pore complex (Gerace and Burke 1988). Nup153 is known to be required for NPC assembly and its anchoring at the nuclear envelope (Walther, Fornerod et al. 2001). Thus, if nuclear pore proteins like gp210 or Nup153 are influenced by viral proteins during the course of infection it will result in disturbance of NPC anchorage. The resulting holes need than to be filled by membrane constituents.

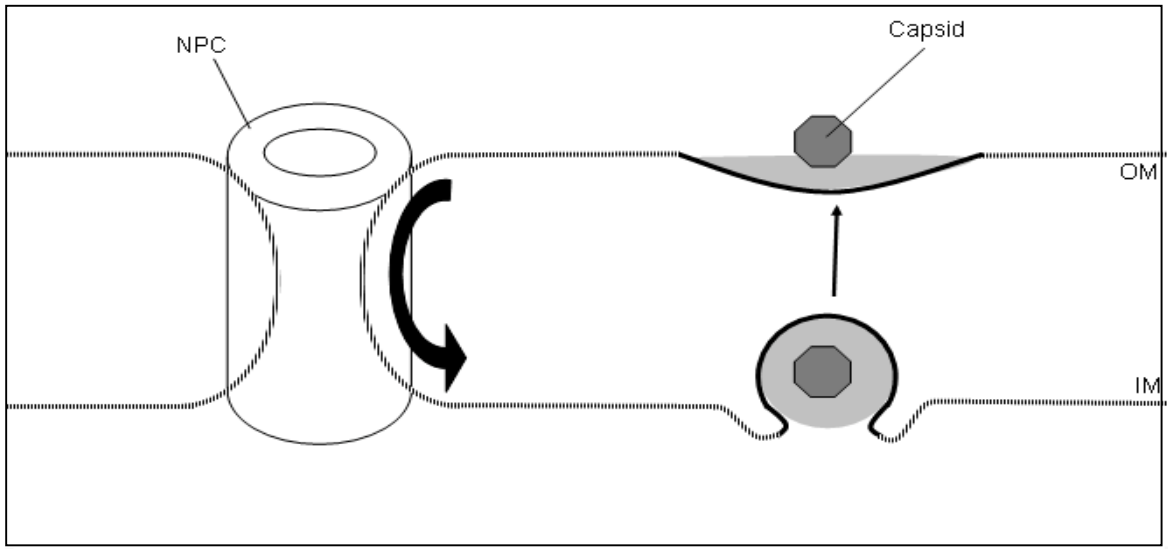


**Fig. 15.** De-envelopment of a capsid at the outer nuclear membrane requires recycling of membrane constituents from the outer to the inner nuclear membrane that would lead to movements of membranes in the area of the nuclear pores.

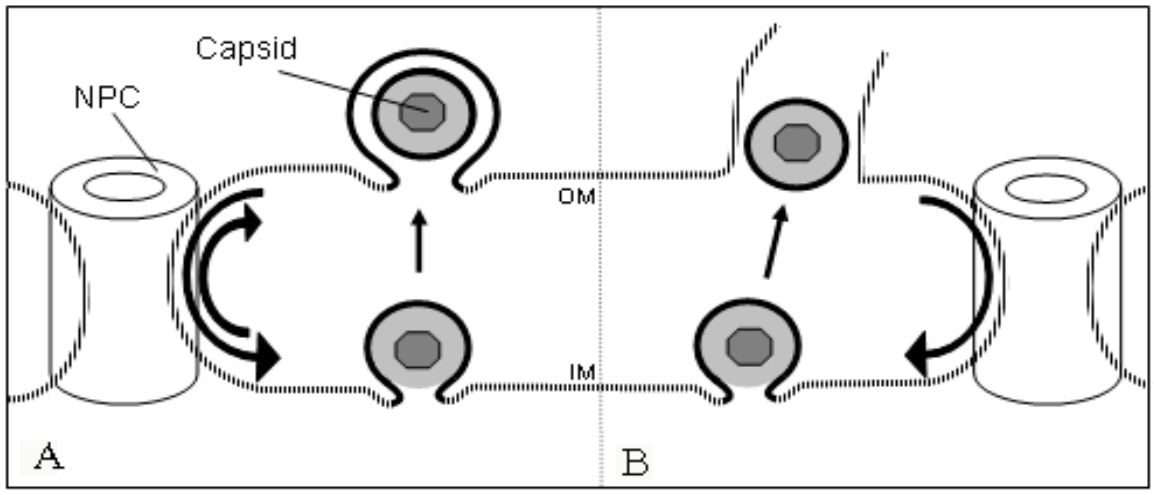


**Fig. 16.** Loss of membranes due to vesicle formation (A) or transportation (B) of virions within the perinuclear space-RER compartment to the Golgi complex

must be replaced either by insertion of membrane constituents from other cellular sites or by de novo synthesis.

### 5.5 Impairment of the Nuclear Pores

Distortion of nuclear pores involving the loss of nuclear pore complexes and enlargement of pore diameter from 140 to 1'900 nm while the nuclear membranes remained intact in BoHV-1 infected MDBK cells have been discovered (Wild, Engels et al. 2005). Apart from impaired nuclear pores the nuclear surface was intact. Indication for nuclear pore impairment was also evident in HSV-1 infected Vero cells (Leuzinger, Ziegler et al. 2005). In this study, nuclear pore diameters were observed to be dilated up to 570 nm by cryo-FESEM in HSV-1 infected HeLa cells.

The fate of NPCs was analysed by confocal microscopy. Nuclear pore proteins p62, p90 and p120 were labelled. Indeed, irregular distribution of the fluorescence signal and building of clusters at the nuclear periphery after 6 h of incubation was demonstrated. These results suggest that proteins from NPCs accumulate around the nuclear membrane. Therefore, the resulting enlarged pores could become an open gate for capsids to exit the nucleus. The nuclear matrix was found by LTEM to protrude into the cytoplasm through up to 650 nm dilated nuclear pores often accompanying by capsids. The nuclear pores were clearly bordered at least at one side with the inner nuclear membrane continuing into the outer nuclear membrane.

Negatively stained nuclear pores on the surface of a carbon coated cover slip measure 125 nm in diameter and are occupied by the NPC (Pante 1996) which controls nuclear import and export of proteins up to 28 nm (Pante and Aebi 1996). In sections where nuclear membranes were hit perpendicular to the nuclear surface, details of both nuclear membranes and nuclear pores could be visualized by LTEM. In this study, intact nuclear pores measured 65 to 125 nm in cryo-FESEM and in LTEM, 100 to 110 nm of diameter in both mock infected

and HSV-1 infected cells. The discrepancies depend on the used methodology. Shrinking artefacts and section thickness did not allow precise measurements.

### 5.6 Exit of Capsids through dilated Nuclear Pores

Herpes virus DNA replicates in the nucleus. After replication, DNA is translocated into capsid that has a diameter of 125 nm and the form of a T=16 icosahedron (Dong-Hua Chen 2001). Capsids are transported to the nuclear periphery where they bud at the inner nuclear membrane acquiring the envelope and tegument proteins (Granzow, Klupp et al. 2001; Wild, Schraner et al. 2002). Both capsid proteins and tegument proteins have to be imported into the nucleus. In this study, high resolution scanning electron microscopy revealed dilated NPC central channels between 100 and 133 nm in *in situ* dry fractured specimen. NPC diameter was enlarged up to 290 nm width. The questions arise i) is nuclear import affected in HSV-1 infected cells and ii) does the import of proteins for building capsids and teguments depend on functional pore complexes. These questions have not been addressed so far in HSV-1 infected cells. However, Gustin and Sarnow (2001) demonstrated that poliovirus infection of HeLa cells results in a dramatic inhibition of nuclear import and the degradation of NPC components. They speculated that inhibition of nuclear import may attenuate antiviral responses, leading to a more productive replication cycle in vivo. To answer the two questions experiments combining nuclear import assays with import studies of viral proteins have to be done.

### 5.7 Localization of Viral Proteins VP22 and VP16

To clarify whether the insertion of mRFP to the VP26 capsid protein could influence the distribution of nuclear pore proteins, immunolabeling using antibodies against tegument proteins VP16 and VP22 revealed that the insertion of mRFP was found to not disturb the distribution of nuclear pore proteins.

Furthermore, the observed colocalization of VP16 and VP22 demand to pay attention on the distribution of these 2 proteins.

The HSV-1 protein VP22 is a major tegument component of the virus particle (Spear and Roizman 1972; Gibson 1974; Knopf and Kaerner 1980). While the exact role of VP22 during virus infection remains unclear, Elliott and O'Hare (1998) have shown that in cells which actively synthesize VP22, during either transient transfection or virus infection, the protein reorganizes and stabilizes the cellular microtubule network, and as such VP22 is the first animal virus encoded protein shown to possess the properties of a cellular microtubule-associating protein. Thus, not only is VP22 a major structural component of the virus particle, it also exhibits several interesting cellular interactions which may be important to the virus replication cycle (Elliott and O'Hare 1999). The structural function of VP16 has been shown to be absolutely essential for virus assembly (Weinheimer, Boyd et al. 1992), as well as in the virion as an essential structural protein of the tegument, and as a consequence, VP16 is delivered to the cell not in isolation but as part of the infecting multicomponent virion (Elliott, Mouzakitis et al. 1995).

Central to the debate concerning herpes virus maturation pathway(s) is the identification of the tegument assembly site within the cell. It has been demonstrated that at least two HSV-1 tegument proteins localize in the nucleus close to putative sites of capsid assembly, termed assemblons (Ward, Ogle et al. 1996), an observation taken to mean that tegument proteins may assemble into the virus particle within the nucleus. It was also shown by immunofluorescence studies that VP22 and another tegument protein, VP16, colocalize in the cytoplasm rather than in the nucleus of both infected and transfected cells (Elliott, Mouzakitis et al. 1995) suggesting that during coexpression these proteins are targeted to the cytoplasmic compartment. Elliott and O'Hare (1999) suggest that the final envelope of the mature virion is acquired at a cytoplasmic

location, further along the exocytotic pathway from the site of VP22 inclusion into the virion. Elliot, Mouzakitis et al. (1995) demonstrated a strong and stable interaction between VP16 and VP22. In addition, coexpression of the proteins in transfected cells resulted in the relocalization of both proteins from their normal sites to a novel structure situated at the edge of the nucleus which has a defined appearance when viewed by phase contrast microscopy.

Based on these observations, the localization of VP22 and VP16 was analysed. After 10 h p.i. both virus proteins were detectable, largely spread through both the cytoplasm and the nucleus. At 14 h p.i., VP22 was in the nucleus and mainly situated at the periphery of the nucleus. VP16 built clusters located obviously in the cytoplasm. Fewer fluorescence signal of VP16 was detected in the nucleus at this time.

Investigations about the localization of VP22 and VP16 performed by immunogold electron microscopy showed that VP22 were not detected in virus particles in the perinuclear space and were present only in mature extracellular virions. VP16 was demonstrated to be located also in virions in the perinuclear space (Naldinho-Souto, Browne et al. 2006). To verify whether this assumption is true, it must be reinvestigated applying an appropriate methodology such as cryosections. Preliminary results showed that VP22 is a constituent of perinuclear virions (Wild, personal communication).

In this study, a clear localization of VP22 in the cytoplasm as well as in the nucleus was demonstrated by confocal microscopy. This suggests that the site of inclusion of VP22 is not only the cytoplasm. The fact that no VP22 was found in virions in the perinuclear space by immunogold labeling could be due to a poor fixation of the central parts of the cells. Concerning VP16, its localization was mainly in the cytoplasm. However, it has been demonstrated that the tegument can assemble independently of the capsid (Rixon, Addison et al. 1992), so that the signal fluorescence could be due to accumulated tegument proteins, not capsids. As our results do not permit comments about eventual localization in

the perinuclear space further investigations are necessary to clarify the complexity of the virus assembly with its tegument proteins incorporation.

## 5.8 Conclusion

In conclusion, the three surface imaging methods, cryo-FESEM, dry-FESEM and confocal microscopy could visually confirm the dramatic structural alteration of the nuclear pores and of the nuclear envelope in the course of HSV-1 infection. Measurements on electron microscopic images revealed that virions cannot bud at nuclear membranes unless membranes are provided for budding by de novo synthesis with or without antecedent loss of NPCs. Considering impaired nuclear pores, further investigations are necessary to determine whether nuclear import is affected in HSV-1 infected cells and whether import of proteins for building capsids and teguments depend on functional pore complexes.

# 6. REFERENCES


Allen, T. D., Goldberg, M.W. (1993). "High resolution SEM in cell biology." Trends Cell Biol. **3**(203-208).

Allen, T. D., S. A. Rutherford, et al. (1998). "Three-dimensional surface structure analysis of the nucleus." Methods in Cell Biology **53**: 125-38.

Braines, J. D., Weller, S.K., Ed. (2005). Cleavage and packaging of herpes simplex virus 1 DNA. Viral Genome Packaging Machines: Genetics, Structures, and Mechanism. Georgetown, TX, USA, Landes Bioscienes.

Browne, H., S. Bell, et al. (1996). "An endoplasmic reticulum-retained herpes simplex virus glycoprotein H is absent from secreted virions: evidence for reenvelopment during egress." Journal of Virology **70**(7): 4311-6.

Campadelli-Fiume, G., F. Farabegoli, et al. (1991). "Origin of unenveloped capsids in the cytoplasm of cells infected with herpes simplex virus 1." Journal of Virology **65**(3): 1589-95.

Cantieni, D. (2000). Intrazellulärer transport und morphogenese des bovinen herpesvirus 1 (BHV-1). Veterinäranatomischen Insitut. Zürich, Universität Zürich**:** 71.

Card, J. P., L. Rinaman, et al. (1993). "Pseudorabies virus infection of the rat central nervous system: ultrastructural characterization of viral replication, transport, and pathogenesis." Journal of Neuroscience **13**(6): 2515-39.

Church, G. A. and D. W. Wilson (1997). "Study of herpes simplex virus maturation during a synchronous wave of assembly." Journal of Virology **71**(5): 3603-12.

Darlington, R. W. and L. H. Moss, 3rd (1968). "Herpesvirus envelopment." Journal of Virology **2**(1): 48-55.

Dong-Hua Chen, J. J., David McNab, Joyce Mitchell, Z. Hong Zhou, Matthew Dougherty, Wah Chiu, and Frazer J. Rixon (2001). "The Pattern of Tegument-Capsid Interaction in the Herpes Simplex Virus Type 1 Virion Is Not Influenced by the Small Hexon-Associated Protein VP26." Journal of Virology **75**(23): 11863-11867.

Drummond, S. a. T. A. (2004). "Structure, function and assembly of the nuclear pore complex." Symposia of the Society for Experimental Biology **56**: 89-114.

Elliott, G., G. Mouzakitis, et al. (1995). "VP16 interacts via its activation domain with VP22, a tegument protein of herpes simplex virus, and is relocated to a novel macromolecular assembly in coexpressing cells." Journal of Virology **69**(12): 7932-41.

Elliott, G. and P. O'Hare (1998). "Herpes simplex virus type 1 tegument protein VP22 induces the stabilization and hyperacetylation of microtubules." Journal of Virology **72**(8): 6448-55.

Elliott, G. and P. O'Hare (1999). "Live-cell analysis of a green fluorescent protein-tagged herpes simplex virus infection." Journal of Virology **73**(5): 4110-9.

Franke, W. W. (1974). "Structrure, biochemistry and functions of the nuclear envelope." International review of cytology. Supplement **4**: 71-239.

Gerace, L. and B. Burke (1988). "Functional organization of the nuclear envelope." Annual Review of Cell Biology **4**: 335-74.

Gershon, A., L. Cosio, et al. (1973). "Observations on the growth of varicella-zoster virus in human diploid cells." Journal of General Virology **18**(1): 21-31.

Gershon, A. A., D. L. Sherman, et al. (1994). "Intracellular transport of newly synthesized varicella-zoster virus: final envelopment in the trans-Golgi network." Journal of Virology **68**(10): 6372-90.

Gibson, W., Roizmann, B. (1974). "Proteins specified by herpes simplex virus. X. Staining and radiolabeling proerties of B capsid and virion properties in polyacrylamide gels." Journal of Virology **13**: 155-165.
Gilbert, R., K. Ghosh, et al. (1994). "Membrane anchoring domain of herpes simplex virus glycoprotein gB is sufficient for nuclear envelope localization." Journal of Virology **68**(4): 2272-85.
Goldberg, M. W., C. Wiese, et al. (1997). "Dimples, pores, star-rings, and thin rings on growing nuclear envelopes: evidence for structural intermediates in nuclear pore complex assembly." Journal of Cell Science **110**(Pt 4): 409-20.
Gong, M. and E. Kieff (1990). "Intracellular trafficking of two major Epstein-Barr virus glycoproteins, gp350/220 and gp110." Journal of Virology **64**(4): 1507-16.
Granzow, H., B. G. Klupp, et al. (2001). "Egress of alphaherpesviruses: comparative ultrastructural study." Journal of Virology **75**(8): 3675-84.
Granzow, H., F. Weiland, et al. (1997). "Ultrastructural analysis of the replication cycle of pseudorabies virus in cell culture: a reassessment." Journal of Virology **71**(3): 2072-82.
Grunewald, K., P. Desai, et al. (2003). "Three-dimensional structure of herpes simplex virus from cryo-electron tomography." Science **302**(5649): 1396-8.
Gustin, K. E. and P. Sarnow (2001). "Effects of poliovirus infection on nucleo-cytoplasmic trafficking and nuclear pore complex composition." EMBO Journal **20**(1-2): 240-9.
Gustin, K. E. and P. Sarnow (2002). "Inhibition of nuclear import and alteration of nuclear pore complex composition by rhinovirus." Journal of Virology **76**(17): 8787-96.
Haines, H. and R. J. Baerwald (1976). "Nuclear membrane changes in herpes simplex virus-infected BHK-21 cells as seen by freeze-fracture." Journal of Virology **17**(3): 1038-42.
Homman-Loudiyi, M., K. Hultenby, et al. (2003). "Envelopment of human cytomegalovirus occurs by budding into Golgi-derived vacuole compartments positive for gB, Rab 3, trans-golgi network 46, and mannosidase II.[erratum appears in J Virol. Arch. 2003 Jul;77(14):8179]." Journal of Virology **77**(5): 3191-203.
Klupp, B. G., J. Baumeister, et al. (1998). "Pseudorabies virus glycoprotein gK is a virion structural component involved in virus release but is not required for entry." Journal of Virology **72**(3): 1949-58.
Knopf, K. W. and H. C. Kaerner (1980). "Virus-specific basic phosphoproteins associated with herpes simplex virus type a (HSV-1) particles and the chromatin of HSV-1-infected cells." Journal of General Virology **46**(2): 405-14.
Kubitscheck, U. and R. Peters (1998). "Localization of single nuclear pore complexes by confocal laser scanning microscopy and analysis of their distribution." Methods in Cell Biology **53**: 79-98.
Leuzinger, H., U. Ziegler, et al. (2005). "Herpes simplex virus 1 envelopment follows two diverse pathways." Journal of Virology **79**(20): 13047-59.
Maul (1977). "the nuclear and cytoplasmic pore complex. Structure, dynamics, distribution and evolution." International review of cytology. Supplement **6**: 75-186.
Maul, G., Price, J.W., Lieberman, M.W. (1971). "Formation and distribution of nuclear pore complexes in interphase." Journal of Cell Biology **51**: 405-18.
Monier, K., J. C. Armas, et al. (2000). "Annexation of the interchromosomal space during viral infection." Nature Cell Biology **2**(9): 661-5.
Naldinho-Souto, R., H. Browne, et al. (2006). "Herpes simplex virus tegument protein VP16 is a component of primary enveloped virions." Journal of Virology **80**(5): 2582-4.
Pante, N. and U. Aebi (1993). "The nuclear pore complex." Journal of Cell Biology **122**(5): 977-84.
Pante, N. and U. Aebi (1996). "Sequential binding of import ligands to distinct nucleopore regions during their nuclear import." Science **273**(5282): 1729-32.

Pante, N., Aebi, U. (1996). "Molecular dissection of the nuclear pore complex." Critical reviews in biochemistry and molecular biology **31**: 153-199.
Pante, N. and M. Kann (2002). "Nuclear pore complex is able to transport macromolecules with diameters of about 39 nm." Molecular Biology of the Cell **13**(2): 425-34.
Radsak, K., M. Eickmann, et al. (1996). "Retrieval of human cytomegalovirus glycoprotein B from the infected cell surface for virus envelopment." Archives of Virology **141**(3-4): 557-72.
Rixon, F. J., C. Addison, et al. (1992). "Assembly of enveloped tegument structures (L particles) can occur independently of virion maturation in herpes simplex virus type 1-infected cells." Journal of General Virology **73**(Pt 2): 277-84.
Roizman, B. (2001). Herpes simplex viruses and their replication. Fields Virology. D. M. K. B. N. Fields, P.M. Howley. Philadelphia, Lipincott-Raven Publishers.
Roizman, B., Sears, A. E. (1996). Herpes simplex viruses and their replication. Philadelphia, Pa, 3rd ed. Lippincott-Raven.
Roller, R. J., Y. Zhou, et al. (2000). "Herpes simplex virus type 1 U(L)34 gene product is required for viral envelopment." Journal of Virology **74**(1): 117-29.
Schwartz, J. and B. Roizman (1969). "Concerning the egress of herpes simplex virus from infected cells: electron and light microscope observations." Virology **38**(1): 42-9.
Simpson-Holley, M., R. C. Colgrove, et al. (2005). "Identification and functional evaluation of cellular and viral factors involved in the alteration of nuclear architecture during herpes simplex virus 1 infection." Journal of Virology **79**(20): 12840-51.
Skepper, J. N., A. Whiteley, et al. (2001). "Herpes simplex virus nucleocapsids mature to progeny virions by an envelopment --> deenvelopment --> reenvelopment pathway." Journal of Virology **75**(12): 5697-702.
Spear, P. G. and B. Roizman (1972). "Proteins specified by herpes simplex virus. V. Purification and structural proteins of the herpesvirion." Journal of Virology **9**(1): 143-59.
Stoffler, D., B. Fahrenkrog, et al. (1999). "The nuclear pore complex: from molecular architecture to functional dynamics." Current Opinion in Cell Biology **11**(3): 391-401.
Studer, D., M. Michel, et al. (1989). "High pressure freezing comes of age." Scanning Microscopy - Supplement **3**: 253-68; discussion 268-9.
Suntharalingam, M. a. S. R. W. (2003). "Peering through the pore: nuclear pore complex structure, assembly, and function." Developmental Cell 4(6): 775-89.
Sutter, E. (2006). Phospholipid metabolism of HSV-1 infected cells. Veterinär-Anatomisches Institut der Vetsuisse-Fakultät. Zürich, Universität Zürich**:** 41.
Torrisi, M. R., C. Di Lazzaro, et al. (1992). "Herpes simplex virus envelopment and maturation studied by fracture label." Journal of Virology **66**(1): 554-61.
Walther, P. a. M., M (1997). "Double layer coating for field emission cryo-SEM-Present state and applications." Scanning **19**: 343-348.
Walther, P. a. W., E et al. (1995). "Double layer coating for high resolution low temperature SEM." Journal of Microscopy **179**: 229-237.
Walther, T. C., M. Fornerod, et al. (2001). "The nucleoporin Nup153 is required for nuclear pore basket formation, nuclear pore complex anchoring and import of a subset of nuclear proteins." EMBO Journal **20**(20): 5703-14.
Ward, P. L., W. O. Ogle, et al. (1996). "Assemblons: nuclear structures defined by aggregation of immature capsids and some tegument proteins of herpes simplex virus 1." Journal of Virology **70**(7): 4623-31.
Weinheimer, S. P., B. A. Boyd, et al. (1992). "Deletion of the VP16 open reading frame of herpes simplex virus type 1." Journal of Virology **66**(1): 258-69.
Whealy, M. E., J. P. Card, et al. (1991). "Effect of brefeldin A on alphaherpesvirus membrane protein glycosylation and virus egress." Journal of Virology **65**(3): 1066-81.

Wild, P., M. Engels, et al. (2005). "Impairment of nuclear pores in bovine herpesvirus 1-infected MDBK cells." Journal of Virology **79**(2): 1071-83.
Wild, P., E. M. Schraner, et al. (2001). "Enhanced resolution of membranes in cultured cells by cryoimmobilization and freeze-substitution." Microscopy Research & Technique **53**(4): 313-21.
Wild, P., E. M. Schraner, et al. (2002). "The significance of the Golgi complex in envelopment of bovine herpesvirus 1 (BHV-1) as revealed by cryobased electron microscopy." Micron **33**(4): 327-37.
Wozniak, R. a. P. R. C. (2003). "Nuclear pores: sowing the seeds of assembly on the chromatin landscape." Current Biology **13**(24): 970-2.
Zhu, Z., M. D. Gershon, et al. (1995). "Envelopment of varicella-zoster virus: targeting of viral glycoproteins to the trans-Golgi network." Journal of Virology **69**(12): 7951-9.

## DANKSAGUNG

Ich bedanke mich bei:

**Prof. Dr. Peter Wild** für die Überlassung des spannenden Dissertationsthemas und die sehr gute Unterstützung,

**Prof. Dr. Ackermann**, für die Übernahme des Korreferats,

**Elisabeth Schraner** für die fachlichen Erklärungen im Labor und an dem konfokalen Mikroskop,

**Urs Ziegler** für die praktische Unterstützung am REM und für die Erlaubnis die Geräte am anatomischen Insitut verwenden zu dürfen,

**Ester Sutter** und **Claudia Senn** für die grosse Hilfe bei der Laborarbeit,

**Hanspeter Gautschi** für die Einführung und den Gebrauch des REM im Center for Microscopy and Image Analysis,

**Alain Pfammatter** für seine liebevolle Unterstützung und die fachlichen Gespräche,

**Elisabeth und Pierre Manera** für ihre Liebe und Grosszügigkeit. Ich bedanke mich vom ganzen Herzen für eure durchgehende Unterstützung,

**Nana**, meinem Jack Russel für ihre Geduld und ihre ständig gute Laune.

## CURRICULUM VITAE

| | |
|---|---|
| Name: | Céline Lorraine Manera |
| Geburtsdatum: | 26.08.1980 |
| Geburtsort: | Neuenburg |
| Nationalität: | Schweizerin |
| Heimatort: | Lausanne (VD) |

| | |
|---|---|
| 1987 – 1996 | Primar- und Sekundarschule in Le Landeron (NE) |
| 1996 – 2001 | Handelshochschule in Neuchâtel, Maturität Typ E |
| 2001 –2005 | Veterinär-Medizin Studium an der Vetsuisse Fakultät, Universität Zürich |
| Oktober 2005 | Staatsexamen für Tierärzte |
| 2006-2007 | Doktorandin am Veterinär-Anatomischen Institut in Zürich unter der Leitung von Prof. Dr. Peter Wild |
| | Assistentin im Bereich der Lehre in Veterinäranatomie und Histologie (bis Ende Juli 2006) |

19. November 2007